Annu. Rev. Astron. Astrophys. 1997. 35: 267-307
Copyright © 1997 by Annual Reviews. All rights reserved

Reprinted with kind permission from Annual Reviews, 4139 El Camino Way, Palo Alto, California, USA

LOW SURFACE BRIGHTNESS GALAXIES

Chris Impey

Steward Observatory, University of Arizona, Tucson, Arizona 85721
e-mail: cimpey@as.arizona.edu"

Greg Bothun

Physics Department, University of Oregon, Eugene, Oregon 97403
e-mail: nuts@moo2.uoregon.edu

Key Words: physical properties, galaxy morphology, cosmology, luminosity function, quasar absorption

Abstract. The properties of galaxies that are lower in surface brightness than the dark night sky are reviewed. There are substantial selection effects against the discovery of galaxies that are unevolved or diffuse; these systems are missing from most wide-field catalogs. Low surface brightness galaxies make up a significant amount of the luminosity density of the local universe. They contribute substantial but poorly determined amounts to the census of baryons and dark matter. Low surface brightness galaxies are also relevant to the interpretation of quasar absorption lines, and to the understanding of rapidly evolving galaxy populations in the more distant universe. Theories of galaxy formation and evolution must accomodate the properties of these diffuse stellar systems.

Table of Contents

- INTRODUCTION
- THE TRUE POPULATION OF GALAXIES
  - Surface Brightness Selection and Galaxy Visibility
  - The Local Galaxy Luminosity Function
- SURVEYS OF LSB GALAXIES
  - Photographic Surveys
  - CCD Surveys
- THE SIGNIFICANCE OF LSB GALAXIES
  - Light and Matter in the Universe
  - Galaxy Evolution
  - Implications for Quasar Absorption
  - Galaxy Formation
- REFERENCES

1. INTRODUCTION

The Cosmological Principle states that the universe will appear homogeneous and isotropic to a typical observer, but one of the deeper implications of this principle is rarely examined. Observational cosmology is usually probed via catalogs of galaxies. Although much of the universe is dark, galaxies are the prime repositories of shining baryonic matter. Galaxy properties are used to measure the size and shape of the universe; deviations from Hubble flow and image distortions through lensing are used to

map out the dark matter distribution. If galaxies are to be used as effective cosmological probes, then our catalogs must be complete and homogeneous, in accord with the Cosmological Principle. Yet the detectability of galaxies depends very much on the cosmic environment. An observer whose star was in a giant molecular cloud or near the center of an elliptical galaxy would have difficulty discovering external galaxies and so would perceive the universe quite differently from us. Put simply, we only catalog the galaxies we can see.

Observational bias in the selection of galaxies dates back to Messier and Herschel. Galaxies are diffuse objects selected in the presence of a contaminating signal: the brightness of the night sky. Below a certain percentage of the night sky brightness, no galaxy can be detected. Above this limiting isophote, a galaxy must present a large enough angular size to be distinguished from a star. For a given luminosity and radial profile, a galaxy will be visible to the maximum distance at a surface brightness level substantially higher than the limiting isophote. High surface brightness galaxies (HSB) are small because they are intrinsically compact, and low surface brightness galaxies (LSB) are small because they mostly fall below the limiting isophote. The night sky essentially acts as a filter, which when convolved with the true population of galaxies, gives the population of galaxies we observe. This censorship due to surface brightness was first commented on by Zwicky (1957), and was further investigated by Arp (1965) and Disney (1976).

This review deals primarily with low surface brightness (LSB) galaxies in the local universe ($z \lesssim 0.1$). There is no convention for defining low surface brightness; discussion is mostly restricted to galaxies with central surface brightness fainter than 23 B mag arcsec^{-2} . Stellar systems more luminous than $M_B = -14$ are considered; for reviews of LSB dwarf galaxies in the Local Group and beyond, see Ferguson & Binggeli (1994), Irwin & Hatzidimitriou (1995), and Mateo (1996). First, the structural properties of galaxies are summarized, and the influence of surface brightness selection is described. Next, the potential incompleteness of galaxy luminosity functions is considered. Surveys for LSB galaxies are reviewed. We then establish the significance of LSB galaxies for the census of light and matter in the universe, for the formation and evolution of galaxies, and for the statistics of quasar absorption. This historically neglected population has important implications for virtually every aspect of observational cosmology. Unless otherwised noted, $H_0 = 100$ km s^{-1} Mpc^{-1} and $q_0 = 0.5$ is assumed, or results are expressed in terms of $h_{100} = H_0 / 100$.

2. THE TRUE POPULATION OF GALAXIES

2.1. Surface Brightness Selection and Galaxy Visibility

For selecting and cataloging galaxies, the simplest assumption is that galaxies form a univariate distribution in apparent brightness. Figure 1a shows the distribution in apparent brightness and effective suface brightness in B of the galaxies from the Messier catalog and a much larger number of galaxies from the Third Reference Catalog of Bright Galaxies (de Vaucouleurs et al 1991; hereafter RC3). Messier produced a catalog of the most prominent nebulae in the sky, as a guide to stationary objects that comet-hunters should avoid. The intervening two centuries have yielded photographic all-sky galaxy samples that reach apparent brightness that is hundreds of times fainter but not substantially fainter in average surface brightness. Despite the inhomogeneous nature of these samples, these data support the idea of a characteristic surface brightness for galaxies.

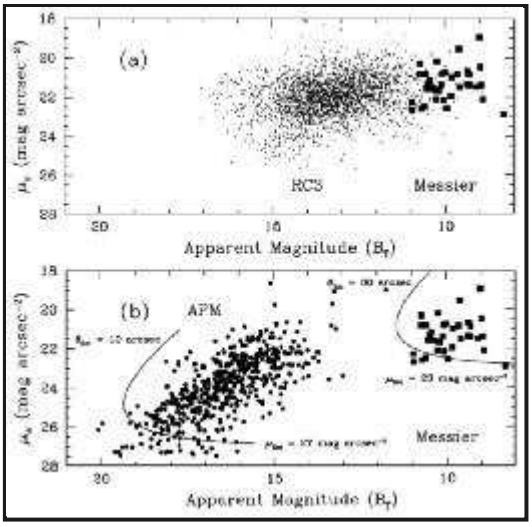

Figure 1. (a) Effective surface brightness in the *B* band plotted against apparent magnitude for Messier galaxies (filled squares) and RC3 galaxies (small dots). (b) Effective surface brightness plotted aginst apparent magnitude for Messier galaxies (filled squares) and LSB galaxies with redshifts from the APM survey (filled circles). The curves show the approximate selection functions for each sample. (From de Vaucouleurs et al 1991, and Impey et al 1996.)

SPECIFYING A GALAXY CATALOG Any galaxy catalog is specified by three parameters: the surface brightness of the limiting isophote ($\mu_{\rm lim}$), the isophotal magnitude limit ($m_{\rm lim}$), and the isophotal size limit in arcseconds at the limiting isophote ($\theta_{\rm lim}$). Assuming symmetric galaxies with no internal absorption, the fraction of the galaxy flux detected above the limiting isophote is

$$S_{\rm lim}/S_{\rm tot} = 1 - \{1 + 0.4\ln 10(\mu_{\rm lim} - \mu_0)\}\ \exp\{-0.4\ln 10(\mu_{\rm lim} - \mu_0)\} \quad (1)$$

for spiral disks and

$$S_{\rm lim}/S_{\rm tot} = 1 - (1 + \sum_{n=1}^{7} \{0.4\ln 10(\mu_{\rm lim} - \mu_0)\}^n/n!) + \exp\{-0.4\ln 10(\mu_{\rm lim} - \mu_0)\} \quad (2)$$

for ellipticals and bulges. The formalism was first presented by Disney & Phillipps (1983). These relations have maxima which occur at $\mu_{\rm lim}$ - μ_0 = 5.37 for spiral disks, and $\mu_{\rm lim}$ - μ_0 = 10.93 for ellipticals, where μ_0 is the central surface brightness.

The observed distribution of galaxy central surface brightness has long been known to be peaked. In the earliest work on the subject, the maximum value for spirals was at μ_0 = 21.6 ± 0.4 mag arcsec^{-2} in *B* (Freeman 1970), and the maximum value for ellipticals was at μ_0 = 14.8 ± 0.9 mag arcsec^{-2} in *B* (Fish 1964). Subsequently, the distributions have been found to be somewhat broader, with a dispersion of $\sigma(\mu_0)$ = 2 mag arcsec^{-2} for spirals (Boroson 1981, van der Kruit 1987, Bosma & Freeman 1993, Courteau 1996), and a dispersion of $\sigma(\mu_0)$ = 1.5 mag arcsec^{-2} for ellipticals (Kormendy 1977). The peaks may reflect an intrinsic property of the galaxy population, a selection effect, or both.

At this point, we make the simplifying assumption that LSB galaxies are suitably described by exponential radial profiles. Late type galaxies are composite stellar systems, where the ratio of disk to bulge flux is $D/B = 0.28(s / r_{\rm e})^2\{(I_0)_{\rm disk} / (I_{\rm e})_{\rm bulge}\}$, where the disk exponential scale length *s* and the bulge effective radius $r_{\rm e}$ are measured in arcseconds. The assumption of exponential profiles is only valid for disk dominated systems, which is appropriate for most deep galaxy surveys. The HST Medium Deep

Survey finds ~ 80% of the *I* band selected sample to be well fit by exponentials (Im et al 1995b). Among low luminosity galaxies, dwarf ellipticals and dwarf irregulars have long been known to have exponential profiles (Binggeli, Sandage & Tarenghi 1984, Gallagher & Hunter 1984). More recently, low luminosity LSB galaxies in clusters have been shown to be well fit by exponential profiles (e.g. Caldwell & Bothun 1987, Impey, Bothun & Malin 1988, Davies, Phillipps & Disney 1990, Bothun, Impey & Malin 1991).

In Figure 1b, the Messier galaxies are compared with the low surface brightness galaxies from a recent survey carried out using Automated Plate Measuring (APM) machine scans of UK Schmidt sky survey plates. This survey is used here to illustrate the issues of surface brightness selection effects, because it is the largest set of field LSB galaxies for which redshifts have been published (Impey et al 1996). The superimposed curves represent the spiral selection function described by equation (1). As surveys probe to smaller fractions of the night sky brightness, the accessible parameter space for detecting galaxies expands. Objects are missed at faint μ_0 owing to the poor contrast with the sky brightness. Objects are missed at faint m_{tot} because they become smaller than the limiting angular size at the limiting isophote. Objects are missed (in principle) at bright μ_0 and faint m_{tot} because they become difficult to resolve from stars.

Practical limitations also exist in the detection of galaxies. For the APM survey, Sprayberry, Impey & Irwin (1996) found 50% completeness for μ_0 = 24 *B* mag arcsec^{-2} and *s* = 10 arcsec, or μ_0 = 23 *B* mag arcsec^{-2} and *s* = 3 arcsec. Photographic amplification of UK Schmidt plates reaches a limiting isophote a factor of two deeper (Malin 1978; Impey, Bothun & Malin 1988). With the new Kodak Technical Pan 4415 emulsion, these limits will become μ_0 = 25.5 mag arcsec^{-2} for *s* = 10 arcsec in the red, or μ_0 = 25 mag arcsec^{-2} for *s* = 3 arcsec again in the *R* band (Schwartzenberg, Phillipps & Parker 1995b). Digital coaddition of scanned films should yield an additional improvement factor of two to three. The detection of faint, extended objects with CCDs is limited by the photon flux and the quality of the flat field. Small scale variations in background can be caused by the detector (i.e. fringing at long wavelengths) or the sky (i.e. faint sources in the sky flat). In practice, it is difficult to achieve flat fields to better than 0.1-0.2% of the sky brightness (Tyson 1988a). In addition, Capaccioli & de Vaucouleurs (1983) have argued that systematic errors preclude reliable surface photometry much fainter than 28 mag arcsec^{-2} . A typical limit for CCD surveys is μ_0 = 27 mag arcsec^{-2} and *s* = 10 arcsec, or μ_0 = 26.5 mag arcsec^{-2} and *s* = 3 arcsec (Schwartzenberg et al 1995a), although galaxy classification is extremely difficult at that level. Phillipps & Disney (1985) have argued that the limit for detecting LSB objects by indirect methods, such as star and galaxy counts, can be as low as 29-30 mag arcsec^{-2} . The lowest backgrounds for the detection of LSB objects are in the vacuum ultraviolet and the near infrared, as seen from space (Wright 1985, O'Connell 1987, O'Neil et al 1996).

GALAXY VISIBILITY The visibility of galaxies is governed by the point at which they are lost from the sample by either falling below the angular size or the flux limit of the survey. Using the expression for the radial intensity profile, the limiting angular diameter at the isophotal limit can be calculated (see Allen & Shu 1979)

$$\theta_{\rm lim} = 1.84 s(\mu_{\rm lim} - \mu_0) \quad (3)$$

and the case of a flux limit is

$$S_{\rm lim} = 2\pi s^2 \mu_0 \{1 - [1 + 0.92(\mu_{\rm lim} - \mu_0)]\, e^{-0.92(\mu_{\rm lim} - \mu_0)}\} \quad (4)$$

We now assume that the number of galaxies observed is proportional to the volume sampled. This implies a survey large enough to include a fair sample of galaxies in the local universe. It also implies that galaxies which cover the full range of structural parameters can be observed at some point in the volume (i.e. no correction factor can be applied for galaxy types which are not detected). In this case $n(\mu_0) \propto \theta_{\rm lim}^{-3}$ for the angular size limit, and $n(\mu_0) \propto S_{\rm lim}^{-3/2}$ for the flux limit. The inevitable consequence of this visibility argument is that the detectability of galaxies is a strong function of surface brightness. The corollary is that the limiting distance to which a galaxy can be observed is a strong function of surface brightness, since $d_{\rm lim} \propto \theta_{\rm lim}^{-1}$ for an angular size limit, and $d_{\rm lim} \propto S_{\rm lim}^{-1/2}$ for a flux limit. Davies (1990) has modelled the visibility of inclined two-component bulge/disk galaxies. Although the selection function no longer has a simple analytical form, the basic features of the more simple treatment are confirmed.

For a catalog with an angular size cutoff, the selection criteria are the isophotal size, $\theta_{\rm lim}$, and the limiting isophote at which that angular size is measured, $\mu_{\rm lim}$. The volume sampled is

$$V(h,\mu_0) \propto s^3(\mu_{\rm lim} - \mu_0) \quad (5)$$

where s and μ_0 are the structural parameters that completely define an exponential profile. For a catalog with a flux limit, the selection criteria are the magnitude limit, $m_{\rm lim}$, and the limiting isophote at which the flux is measured. Since catalogs limited by total flux do not exist, we must also specify $S_{\rm lim}$ / $S_{\rm tot}$, the fraction of the total flux that is measured down to the limiting isophote. Then the visibility volume is

$$V(h,\mu_0) \propto s^3 10^{-0.6(\mu_{\rm lim}-\mu_0^*)}\{1+(1+0.92(\mu_{\rm lim}-\mu_0))\exp(-0.92(\mu_{\rm lim}-\mu_0))\}^{3/2} \quad (6)$$

where μ_0* is a fiducial luminosity analogous to L*, conveniently taken to be the Freeman value. The last two equations reflect the formalism of McGaugh et al (1995); Disney & Phillipps (1983) had previously defined visibility functions in terms of luminosity and surface brightness. Since galaxies are not selected by total magnitude, and the proportion of the galaxy flux detected depends on the surface brightness, it is simpler to deal with the visibility functions defined in terms of structural parameters. As expected, the range of surface brightness for nearby galaxies is substantially larger than for more distant galaxies (Impey et al 1996). This is exactly as expected under the influence of surface brightness selection, where galaxies of intermediate surface brightness can be seen to the largest distances (see also Phillipps, Davies & Disney 1990). Regardless of whether the catalog is limited by angular size or isophotal flux, the visibility increases monotonically with larger scale length and brighter surface brightness. The volume sampling functions are very steep; the volume over which low surface brightness galaxies can be observed is small, so the correction to the space density is correspondingly large.

THE INTRINSIC SURFACE BRIGHTNESS DISTRIBUTION The intrinsic surface brightness distribution can only be recovered if a survey has selection parameters $\mu_{\rm lim}$, $m_{\rm lim}$, and $\theta_{\rm lim}$ which have been rigorously applied to the catalog. McGaugh (1996) has applied these methods to several samples, notably the diameter-limited Fornax catalog of Davies (1990), and has shown that the presumption of a preferred surface brightness at the Freeman value is clearly invalid. The distribution function cuts off sharply at high surface brightness, but it has a long tail that is populated down the faintest detectable galaxies. The lack of high surface brightness disk galaxies is real and not a selection effect. Below $\mu_0 \approx$ 21.5 mag arcsec^{-2} , the numbers fall to about one fourth to one fifth of the peak at $\mu_0 \approx$ 23.5 mag arcsec^{-2} , but there is no sign of a sharp turndown. No cutoff in the surface brightness distribution has been found down to the limit of deep CCD surveys, μ_0 ~ 26 mag arcsec^{-2} (Schwartzenberg et al 1995a, Dalcanton 1995).

The studies just referred to do not have redshifts, so they must make the implicit assumption of a separable bivariate luminosity function, $\Phi(s,\mu)$, ie. that scale length and central surface brightness are not correlated. The surveys of de Jong (1995) and Impey et al (1996) do not have to make this assumption since redshifts allow absolute scale lengths to be calculated. For the APM sample, the detection probability as a function of μ_0 and s was estimated, and the observed distribution $n(\mu_0)$ was corrected for this incompleteness. For the raw data, $< V / V_{\rm max} > = 0.18 \pm 0.06$. After weighting by the inverse probability of detection, $< V / V_{\rm max} > = 0.44 \pm 0.06$, which is consistent with completeness brighter than $\mu_0 = 25$ B mag arcsec^{-2} , above which the corrections become very large and uncertain. The result is a distribution with a broad peak at $\approx$ 21.5 mag arcsec^{-2} , which falls by a factor of 4-5 by $\mu_0 \approx$ 23.5 mag arcsec^{-2} , but then continues with with no sign of a cutoff (Sprayberry et al 1996). The result is inconsistent with the traditional description of a Gaussian distribution of surface brightness. The number of disk galaxies falls slowly as a function of μ_0, but with no limit apart from that imposed by observational selection.

2.2. The Local Galaxy Luminosity Function

The luminosity function of galaxies is fundamental to observational cosmology. As emphasized by Binggeli, Sandage & Tammann (1988), there is no universal luminosity function; the space density of galaxies is a function of Hubble type and the density of the environment. Accurate knowledge of the luminosity function is required to test cosmological world models and to understand galaxy evolution. Presumably, the shape of the luminosity function also contains "frozen in" clues to the process of galaxy formation. For example, if Freeman's law for spiral disks is correct there is only one parameter relevant to galaxy selection, as only variations in size act to modulate variations in luminosity. This would require all the physical processes of galaxy formation and evolution to conspire to result in one specific value of central surface brightness for all galaxies.

THE GALAXY LUMINOSITY FUNCTION The parametrization of the number of galaxies per unit volume according to Schechter (1976) is

$$\phi(L)dL = \phi^*(L/L^*)^{\alpha}e^{-L/L^*}d(L/L^*) \quad (7)$$

where Φ^* characterizes the space density of galaxies, L^* is the luminosity above which galaxies are rare, and α is the asymptotic slope of the faint end of the luminosity function.

Field luminosity functions in the local universe were first reviewed by Felten (1977), and Binggeli, Sandage & Tammann (1988). More recently, large photographic surveys have been used to define the local luminosity function with better statistics. Efstathiou, Ellis & Peterson (1988) found $\Phi^* = 0.016$, $M^* = -19.7$, and $\alpha = -1.07$. Loveday et al (1992) found $\Phi^* = 0.014$, $M^* = -19.5$, and $\alpha = -0.97$ for the Stromlo-APM survey. Marzke, Huchra & Geller (1994a) found $\Phi^* = 0.010$, $M^* = -18.8$, and $\alpha = -1.07$ for the Center for Astrophysics survey, and da Costa et al (1994) found $\Phi^* = 0.015$, $M^* = -19.5$, and $\alpha = -1.20$ for its southern equivalent, the Southern Sky Redshift Survey. The first extensive field galaxy survey to be selected from CCD images is the Las Campanas Redshift Survey; Lin et al (1996) present the parameters $\Phi^* = 0.019$, $M^* = -20.3$, and $\alpha = -0.70$. For the photographic surveys, M^* is measured in absolute B magnitudes; the Las Campanas survey used Gunn-r band selection. All surveys quote L^* in the equivalent in solar units, and the normalization Φ^* in units of h^3_{100} Mpc^{-3} mag^{-1}. Note that these recent determinations differ by more than a factor of two in both normalization, Φ^*, and characteristic luminosity, M^*. See also the discussion by Ellis in this volume.

THE FAINT END SLOPE IN CLUSTERS AND THE FIELD The faint end slope of the galaxy luminosity function is most easily studied in nearby clusters, where cluster membership can be decided with reasonable reliability in the absence of redshifts, using morphology and two dimensional spatial distribution as a guide.

Sandage, Binggeli & Tammann (1985) revealed the existence of large numbers of faint galaxies in the Virgo cluster. Ferguson & Sandage (1988) followed that work up with a similar survey of the Fornax cluster, deriving a faint end slope of $\alpha \approx -1.3$ for both clusters. Correcting for surface brightness selection effects, Impey, Bothun & Malin (1988) deduced $\alpha \approx -1.6$ for the Virgo cluster, and Bothun, Impey & Malin (1991) found $\alpha \approx -1.5$ for the Fornax cluster. Tyson & Scalo (1988) postulated a large population of gas-rich dwarfs that could substantially steepen the luminosity function. In both clusters, the population that steepens the luminosity function has low luminosity ($M_B > -16$), moderate scale length (3-10 kpc), and low surface brightness ($\mu_e > 25$ B mag arcsec^{-2}). These studies were all based on photographic material. CCD surveys have advanced our census of intrinsically faint galaxy populations. The dwarf luminosity function in Abell 963 has an overall slope of $\alpha \approx -1.8$ (Driver et al 1994a), Bernstein et al (1995) observed a faint end slope of $\alpha \approx -1.4$ in the core of the Coma cluster, and Trentham (1997) found slopes of $-1.8 < \alpha < -1.6$ for three spiral-rich, poor clusters. The latter two results reach down to the luminosity of the Local Group dwarf spheroidals. With smaller samples and a less secure background correction, de Propris et al (1995) find even steeper slopes for four rich Abell clusters, $\alpha \approx -2.2$.

A magnitude limited redshift survey must sample several thousand galaxies to include a few dozen fainter than $M^* + 5$. Our knowledge of the field galaxy luminosity function fainter than $M_B = -16$ is poor for two reasons. Shallow, wide-field surveys have small effective volumes for the detection of low luminosity systems. Also, regardless of the exact relationship between luminosity and surface brightness, magnitude limited redshift surveys must be increasingly censored by surface brightness selection effects at $M_B > -16$.

Driver & Phillipps (1996) find the Stromlo-APM survey to be entirely consistent with a faint end slope of $\alpha = -1.5$. A reanalysis of the CfA redshift survey by Marzke et al 1994b) suggests that the faint end slope is as high as -1.85 for low luminosity spirals and irregulars. Marzke & da Costa (1997) deduce a Schechter function with $\alpha = -1.5$ for the blue galaxies ($B - R < 1.3$) in the Southern-Sky Redshift Survey, and the deepest part of the sample yields a slope as steep as $\alpha = -1.7$. The ESO Slice Survey has also been compared directly to the Stromlo-APM survey by Zucca (1997), who finds a higher normalization than Loveday et al (1992), and a faint end with $\alpha = -1.6$ due entirely to LSB and compact star-forming galaxies. An extension of the Las Campanas Redshift Survey to correct for excluded LSB galaxies also results in a steeper faint end slope (JJ Dalcanton and SA Schectman, in preparation). Bershady et al (1997) have carried out a local ($z < 0.1$) *UBVRI* survey down to $\mu_B = 24.5B$ mag arcsec^{-2} over 1 deg^2, and find blue field galaxies to have a steep slope of $\alpha = -1.6$. The Texas Deep Sky Survey is a *UBVRI* survey covering 50 deg^2 that will reach $\mu_B = 23.5B$ mag arcsec^{-2} . These multicolor CCD surveys are deep enough to detect LSB galaxies that are missing from most photographic catalogs.

The data in both clusters and the field appear to be best described by a composite luminosity function. Giant galaxies, especially those of early type with high surface brightness, have either a conventional Schechter function with $\alpha = -1$ to -1.1 or a Gaussian luminosity function. Dwarf galaxies, especially those of late type with low surface brightness, have steep Schechter slopes of $\alpha = -1.5$ to -2 which begin to dominate at $-15 < M_B < -17$. A single Schecter function is a poor description of almost any survey that spans more than six magnitudes in luminosity. The steep faint end slope has so far been most clearly seen in poor,

spiral-rich clusters or in samples of blue field galaxies. We note that in the case where α = - 1.5, $L_{tot} \simeq 1.8\Phi^* L^*$ and the number of galaxies per luminosity interval is $dN = \Phi^* exp(-L/L^*) dL / L^*$. The steep luminosity function at the faint end for gas-rich dwarfs was first proposed by Tyson & Scalo (1988), and has been argued for on different grounds by Schade & Ferguson (1994).

RECOVERING THE TRUE GALAXY POPULATION Correct calculation of a luminosity function requires a measurement of the bivariate distribution of luminosity and surface brightness. The luminosity should be calulated from a total rather than an isophotal magnitude. Most constructions of the luminosity function implicitly assume a delta function surface brightness distribution, and no published luminosity function has made corrections for surface brightness selection effects. Figure 2 shows how significant the addition of diffuse galaxies can be. The RC3 galaxies form a broad distribution around a characteristic value of μ_e = 22 mag arcsec^{-2} in B; optical and/or 21 cm redshifts have been measured for all the LSB galaxies plotted in Figure 2. With a fainter limiting isophote, the APM survey recovered previously uncataloged galaxies down to μ_e = 26 mag arcsec^{-2} . The correlation between total luminosity and surface brightness has a very large scatter. Over the range 23 < μ_e < 25, galaxies are being discovered over the entire range -14 > M_B > - 21. The far left solid curve of Figure 2 represents the selection function at 50% completeness.

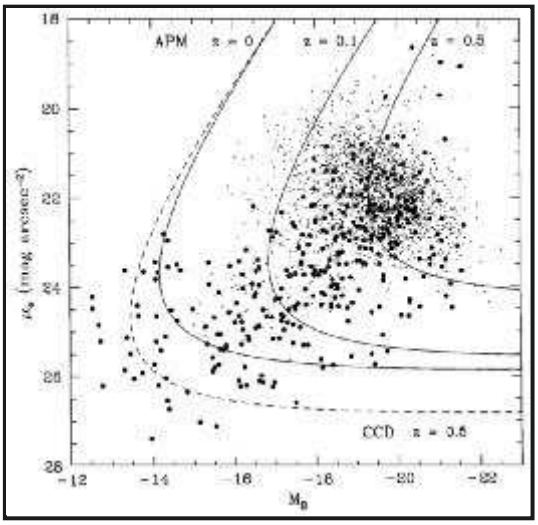

Figure 2. Effective surface brightness plotted against blue luminosity for RC3 galaxies (small dots) and LSB galaxies from the APM survey (large dots). The correlation between luminosity and surface brightness for the LSB galaxies is weak. (From de Vaucouleurs et al 1991 , and Impey et al 1996 .) The three solid curves show the APM selection function, assuming μ_{lim} = 26 B mag arcsec^{-2} and θ_{lim} = 10 arcsec. The dashed curve is the selection function from the pencil beam CCD survey of Lilly (1993) , assuming limits of μ_{lim} = 28.6 B mag arcsec^{-2} and θ_{lim} = 2 arcsec.

The derivation of a luminosity function is complicated by the correlation between surface brightness and luminosity. Rather than calculate $n(L, \mu)$, it is possible to calculate $n(I_0, s)$, since I_0 and s uniquely define luminosity and they are observed to be uncorrelated for low surface brightness galaxies fit by exponentials. In this case

$$n(L)dL = 2\pi \int_{s_{min}}^{s_{max}} \int_{I_{min}}^{I_{max}} I_0^{-p} s^{-2q} dI_0 ds \quad (8)$$

where the distributions of structural parameters, after correction for selection effects, are $n(I_0) \propto I_0^{-p}$ and $n(s) \propto s^{-q}$. Assuming that this double integral is bounded by the observed upper limits on central surface brightness and scale length $n(L) \propto$ [1 - (L /

$L_{max})^{1-p}][1 - (L / L_{max})^{(1-2q)/2}]$, which reduces to $n(L) \propto L^{-1.5}$, if $p \approx 1$ and $q \approx 2$, as observed. As noted by Phillipps & Driver (1995), $n(L)\, dL \propto \int I_0^{-1}(I_0 / L)(I_0 L)^{-1/2}\, dI_0 dL$, which reduces to $n(L) \propto L^{-3/2}(I_{max}^{1/2} - I_{min}^{1/2})$, and so the fraction of galaxies above I_{min} is $1 - (I_{min} / I_{max})^{1/2}$, independent of luminosity.

Sprayberry et al (1997) have compared the APM survey of LSB galaxies directly to the CfA redshift survey. By measuring the surface brightness properties of the CfA galaxies, a volume limited sample of LSB galaxies with redshifts can be defined that has no overlap with the CfA survey (ie. $\mu_0 > 22$ mag arcsec^{-2}). The predominantly late-type low surface brightness galaxies in the range $22 < \mu_0 < 25$ B mag arcsec^{-2} are at least as numerous as the late-type CfA galaxies presented by Marzke et al (1994b). The amount of extra luminosity density is 25-30%. Because the number distribution is nearly flat down to the lowest surface brightness reached by the APM survey, these are lower bounds to the missing LSB population. Using the maximum liklihood estimator of Sandage, Tammann, & Yahil (1979), a Schechter function for the giants, and a power law function for the dwarfs, the luminous galaxies are fit by a standard slope of $\alpha = -0.9$, and the dwarfs have a steeper (but more uncertain) slope of $\alpha = -2.2$. It is not known how this analyis would be affected by the addition of galaxies at even fainter suface brightness levels of $\mu \sim 27$ mag arcsec^{-2} , such as have been discovered in CCD surveys (Dalcanton 1995).

To summarize, the local galaxy luminosity function cannot be derived without correcting for surface brightness selection effects. These effects are more severe for late type and gas-rich galaxies than for early type and gas-poor galaxies, because the latter have generally higher surface brightness and a tighter correlation between luminosity and surface brightness (Binggeli, Sandage, & Tarenghi 1984). Isophotal magnitudes generally measure a smaller fraction of the total galaxy flux as the surface brightness decreases. Procedures that assume that each luminosity interval has a similar distribution of surface brightness, or that S_{lim} / S_{tot} is not a function of surface brightness, may be in error. For galaxy types where the correlation between luminosity and surface brightness has large scatter, the corrections are substantial. The volume corrections are largest for the faintest galaxies, where the numbers in local surveys are fewest, and where the incompleteness corrections are largest. When these corrections are made to shallow wide-angle surveys, or when considering deep pencil-beam surveys which tend to have fainter isophotal limits, the slope of the tail of the luminosity function is at least as steep as $\alpha = -1.4$. By far the most ubiquitous type of galaxy in the universe is the low surface brightness dwarf. These galaxies are almost completely missing from published local luminosity functions.

3. SURVEYS OF LSB GALAXIES

Over the past 15 years, a number of surveys have succeeded in locating low surface brightness galaxies. The distribution in surface brightness is continuous, but operationally we choose to define galaxies with $\mu_0 \geq 23$ mag arcsec^{-2} as low surface brightness. In terms of the narrow surface brightness distribution of Freeman (1970), a disk galaxy this diffuse should be extremely rare. In practice, low surface brightness galaxies are a mixed bag, including objects as diverse as giant gas-rich disks and dwarf spheroidals. This of course is the reason for their importance: such galaxies offer a new window onto the diversity of galaxy morphology and evolution.

3.1. Photographic Surveys

Unsurprisingly for someone who left his idiosyncratic mark on much of extragalactic astronomy, Zwicky (1957) was one of the first to speculate on the existence of low surface brightness galaxies. His claim of a steeply inceasing tail of faint galaxies was at odds with Hubble's (1936) earlier Gaussian form for the luminosity function. In retrospect, both were correct; Hubble had identified mostly galaxies of high surface brightness, Zwicky had discovered an exponential tail of mostly low surface brightness dwarfs. The David Dunlap Observatory (DDO) catalog (van den Bergh 1959) was the first catalog to contain significant numbers of diffuse galaxies, although most of them had low mass and so were not representative of the full range of LSB types. Meanwhile, Reaves (1956) and Arp (1965) had identified the selection effect which might lead low surface brightness galaxies to be missed. This selection bias was first clearly formulated by Disney (1976).

The discovery of low surface brightness galaxies advanced considerably in the 1980s. In a prescient piece of work, Longmore et al (1982) obtained optical and 21 cm data on a sample of 151 LSB galaxies selected by visual inspection of UK Schmidt plates. Many early studies were based on the diameter limited Uppsala General Catalog of Galaxies (UGC; Nilson 1973). With no explcit surface brightness selection, the UGC contains for example an order of magnitude more LSB galaxies than the catalog of Fisher & Tully (1981). LSB galaxies from the UGC catalog were subsequently studied by Romanishin et al (1982), who noted that they had relatively large amounts of gas for their luminosity.

Large numbers of LSB dwarfs were detected in the monumental photographic survey of the Virgo cluster by Binggeli, Sandage, & Tammann (1985) using plates taken with the Du Pont 100-inch telescope. Another large survey was carried out in the nearby Fornax cluster using both du Pont plates (Ferguson & Sandage 1988, Ferguson 1989) and sky survey plates from the UK

Schmidt Telescope (Phillipps et al 1987). The surface brightness limits of both these surveys were $\mu_{lim} \approx 25$ *B* mag arcsec^{-2}, however the spatial resolution and morphological classification is superior on the du Pont plates, which gives an advantage in defining cluster membership in the absence of redshifts.

The next improvement was offered by visual searches of the POSS-II plates, which reach to a deeper limiting isophote, $\mu_{lim} \approx 26$ *B* mag arcsec^{-2} (Schombert & Bothun 1988, Schombert et al 1992). Binggeli, Tarenghi & Sandage (1990) used deep Palomar plates to identify several hundred predominantly LSB dIm and dE galaxies. Impey, Bothun & Malin (1988) used photographically amplified images of Virgo to push the limiting isophote down to $\mu_{lim} \approx 27.5$ *B* mag arcsec^{-2}, and a similar surface brightness can be reached by automated scans of UK Schmidt plates (Irwin et al 1990a). These studies yielded new samples of extremely LSB galaxies in Virgo and Fornax (Davies et al 1988; Bothun, Impey & Malin 1991). A further gain in sensitivity can be achieved by digitally stacking scans of existing sky survey plates, or by using Tech Pan emulsions; large-scale surveys are currently underway with limits of $\mu_{lim} \approx 27$ *R* mag arcsec^{-2} (Schwartzenberg, Phillipps & Parker 1995b).

3.2. CCD Surveys

Digital detectors can survey for LSB galaxies in the field down to a much lower limiting isophote, but over much smaller areas (Schwartzenberg et al 1995a). CCD surveys of nearby (Turner et al 1993, Bernstein et al 1995) and more distant clusters have been undertaken (Driver et al 1994). The Texas Survey for field LSB galaxies adds a new dimension with red selection down to $\mu_{lim} \approx 27.5$ *R* mag arcsec^{-2} (O'Neil et al 1997). Dalcanton et al (1997b) have used strip scans made with the Palomar 200-inch telescope operating in transit mode to find galaxies with $23 < \mu_0 < 27$ *V* mag arcsec^{-2}. This approaches the limit below which individual galaxies cannot be distinguished from distant clusters of galaxies (Schectman 1973). At the limit of deep surveys, LSB galaxies are being mined from the WFPC2 images of the Hubble Deep Field by several groups. The next major step forward in large area surveys will come with the Sloan Digital Sky Survey (Gunn & Knapp 1993).

The diversity of galaxies uncovered by these surveys is striking. An early surprise was the accidental discovery of the giant LSB disk galaxy Malin 1 in a survey of the Virgo cluster (Bothun et al 1987). This remarkable galaxy is the prototype of systems which have low surface mass density stellar disks, large physical sizes, and enormous amounts of neutral hydrogen (Impey & Bothun 1989, Knezek 1993). These galaxies are extreme cousins of the gas-rich LSB galaxies discussed by Longmore et al (1982), characterized by large exponential scale lengths ($s > 10$ kpc) and low central surface brightnesses ($\mu_0 > 25$ *B* mag arcsec^{-2}). Further examples have recently been found (Bothun et al. 1990, Sprayberry et al. 1993, 1995a). Dwarf spirals have also been detected (Schombert et al 1995); both the smallest and the largest spiral galaxies known have low surface brightness. At the other extreme are LSB dwarfs, with similar surface brightness but much smaller scale lengths ($s \sim$ 1-2 kpc). Surface brightness selection accounts for the fact that dwarf members of the Local Group continue to be discovered (Irwin et al 1990b). Even at the modest distance of the Coma cluster, many Local Group dwarf spheroidals would be too low in surface brightness to be detected in a shallow survey, and too compact to be distinguished from stars in a deep survey.

4. THE SIGNIFICANCE OF LSB GALAXIES

Our ignorance of the true galaxy population affects virtually every aspect of observational cosmology. Study of the detailed properties of galaxies is confined to nearby, prominent examples. Beyond the Milky Way, most of our information on the stellar populations, kinematics, dark matter content, star formation history, and large scale clustering of galaxies is based on studies of high surface brightness objects. Without accounting for LSB galaxies, we cannot complete a census of the luminous density and matter content of the universe.

4.1. Light and Matter in the Universe

There are reasons to believe that the existing census of galaxies is incomplete. Figure 3 shows current constraints on luminous and nonluminous material in the universe. The left-hand panel shows the integrated surface intensity of the galaxy counts down to $V = 27$ (Tyson 1995). The sum is dominated by counts well above the magnitude limit of the survey, and this is nearly an order of magnitude lower than the upper bound on the extragalactic part of the diffuse sky brightness (Mattila 1990). The center panel of Figure 3 shows HI column density, where bright spirals have a peak HI column density in the range $5 \times 10^{20} < N_{HI} < 2 \times 10^{21}$ atoms cm^{-2} (Warmels 1985, Cayette, Kotanyi & Balkowski 1993). At lower HI column densities, $3 \times 10^{20} < N_{HI} < 8 \times 10^{20}$ atoms cm^{-2}, the efficiency of star formation is greatly reduced (Kennicutt 1989, van der Hulst et al 1993). At still lower column densities, disks may be ionized, and such diffuse gas clouds may not be detectable with HI surveys (Maloney 1993).

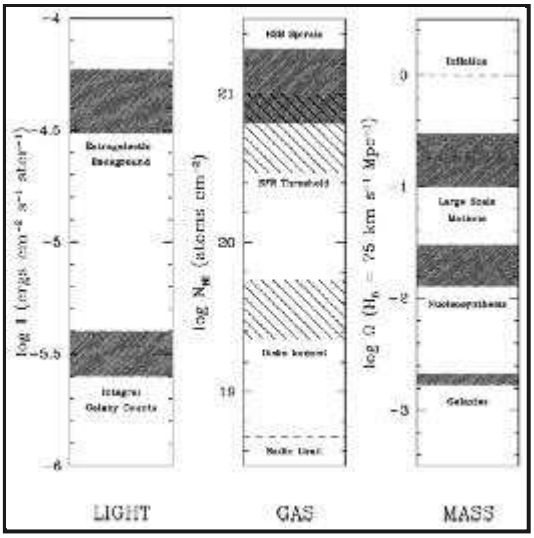

Figure 3. The left panel shows the intensity of diffuse extragalactic light. The integral of the faint galaxy counts (Tyson 1995) is nearly an order of magnitude below the observations upper bound (Mattila 1990). The center panel shows the HI column density of gas in galaxies.
Superimposed are the range of column densities for normal luminous spirals (Cayette, Kotanyi & Balkowski 1993), the range of the threshold column density below which star formation is inefficient (Kennicutt 1989), and the probable column density at which disks in the local universe are ionized (Maloney 1993). The right panel shows mass components in the universe as a fraction of the critical density. The upper band is the range from large scale motions (e.g. Peebles 1993), the middle band is the rang from nucleosynthesis arguments (Walker et al 1991), and the lower band is the observed contribution in luminous galaxies (Persic & Salucci 1992).

The right-hand panel of Figure 3 shows various measures of the mean mass density, Ω_0. The agreement between the observed abundances of light elements and the predictions of primordial nucleosynthesis is one of the great successes of standard cosmology (Walker et al 1991). Yet, a careful accounting of the visible material in and between galaxies shows that it falls short of matching the amount of baryonic material predicted by the big bang model (Persic & Salucci 1992). For an allowed range of nucleon densities, $2.8 \times 10^{10} < n_{\rm baryon} / n_\gamma < 4.0 \times 10^{10}$, Walker et al (1991) find the constraint on the baryon density parameter to be $0.010 < \Omega_{\rm baryon}\, h_{100}^2 < 0.015$.

The visible contribution from baryons is given by the sum $\Omega_{\rm baryon} = \Omega_{\rm E/S0} + \Omega_{\rm Sp} + \Omega_{\rm clusters} + \Omega_{\rm groups}$, where the results of the Gunn-Peterson test put a very low limit on any diffuse component of cold intergalactic hydrogen. The inventory by Persic & Salucci (1992) yields a total of $\Omega_{\rm baryon} = (2.2 + 0.6 h_{100}^{-3/2}) \times 10^{-3}$, so that most baryons must be dark for $0.5 < h_{100} < 1$. X-ray observations of rich clusters imply $\Omega_{\rm baryon} / \Omega_{\rm tot} \sim 0.1$-$0.3$ (e.g. White et al 1993). Since inhomogeneous nucleosynthesis cannot be used to raise the baryon density above $\Omega_{\rm baryon} \sim 0.1\, h_{100}^2$ (Malaney & Mathews 1993), this observation is difficult to understand unless the standard scenario of a flat universe is incorrect; see the extensive discussion of baryonic dark matter by Carr (1994).

LUMINOSITY DENSITY For cosmological purposes, the integrated luminosity density is more important than the integrated number density. It is also a more robust way of comparing galaxy samples than by Schechter function parameters (assuming that the integral has converged 3-4 magnitudes (mag) below L*, when the incompleteness of most samples becomes large). For the CfA survey (Marzke et al 1994a),

$$L_{\rm tot} = \int\int \phi(L,\mu_0) L dL d\mu_0 = 11 \pm 4 \times 10^7 h_{100}\ L_\odot {\rm Mpc}^{-3} \quad (9)$$

A variation of nearly a factor of two is seen between this and other published values for the luminosity density; Efstathiou et al (1988) found $19 \pm 7 \times 10^7\ h_{100}\ L_\odot\ Mpc^{-3}$, Loveday et al (1992) found $15 \pm 3 \times 10^7\ h_{100}\ L_\odot\ Mpc^{-3}$, and Lin et al (1996) found $19 \pm 1 \times 10^7\ h_{100}\ L_\odot\ Mpc^{-3}$. From the APM survey of late-type LSB galaxies, Sprayberry et al (1997) derive $3 \pm 0.5 \times 10^7\ h_{100}\ L_\odot\ Mpc^{-3}$. This exceeds the luminous density of late type irregulars found by Marzke et al (1994a), and is 15-30% of the luminous density for all morphological types found by all investigators. Dalcanton et al (1997a) reached similar conclusions based on a smaller number of redshifts from a CCD survey; LSB galaxies contribute 10-100% of the luminous density seen in HSB galaxies. The LSB correction to the luminosity density is only valid over the range $22 < \mu_0 < 25$ mag arcsec^{-2}, and this correction must be a lower limit because the surface brightness distribution is nearly flat down to the limits of current observations.

EXTRAGALACTIC BACKGROUND LIGHT The extragalactic background light (EBL) is an integral sum of the star formation history of the universe, more sensitive in practice to galaxy evolution than to the parameters of the cosmological model (Harrison 1964). It also provides a fundamental limit to the potential profusion of LSB galaxies. The observed upper limit on the diffuse EBL is subject to the accurate elimination of foreground components that are several hundred times larger; Mattila, Leinart & Schnur (1991) summarize a number of measurements which yield upper limits in the range $4.5\text{-}10 \times 10^{-9}$ *erg cm*$^{-2}$ *s*$^{-1}$ *ster*$^{-1}$ Å^{-1}. The integral of the number counts of galaxies down to a *B* band isophote of 30 mag arcsec^{-2} (Tyson 1995) is

$$I_{\rm EBL} = \int_m^\infty N(m) 10^{-0.4(m+20.45)} dm = 6.4^{+0.2}_{-0.1} \times 10^{-10} {\rm ergs\ cm^{-2} s^{-1} sr^{-1} \AA^{-1}} \quad (10)$$

The corresponding number from the survey of Cowie, Hu & Songaila (1995b) is 4×10^{-10} *erg cm*$^{-2}$ *s*$^{-1}$ *ster*$^{-1}$ Å^{-1}. These measurements with their uncertainties are shown in the left panel of Figure 3.

The existing limits on the EBL allow for large populations of LSB galaxies; note, however, that they are not present in large numbers in the deep CCD data (Tyson 1995). Väisänen (1996) concluded that populations of LSB galaxies permitted by the number counts can raise the EBL by a factor of 2-3. Models which include large numbers of LSB dwarfs lead to a predicted EBL within a factor of two of the current limit (Ferguson & McGaugh 1995, Morgan & Driver 1995). Depending on the evolution model assumed, the steep faint end tail of the local luminosity function discussed previously would not contribute to the pencil-beam counts until $B \sim 26$, substantially fainter that the level of the peak contribution of the counts to the EBL, $B \sim 24$. Since LSB galaxies are largely quiescent, their existence in large numbers would not violate the constraint that we have already identified the sources of most of the metal production in the universe (Cowie 1988). The directly meaured contribution of LSB galaxies from the APM survey is 2×10^{-10} *erg cm*$^{-2}$ *s*$^{-1}$ *ster*$^{-1}$ Å^{-1}, or 30-50% of the amount from the integral number counts.

A separate constraint comes from the fluctuations in the EBL (Schectman 1974). Note that LSB galaxies can add to the level of the EBL without increasing the amplitude of the fluctuations, because they are observed to be weakly clustered (Mo, McGaugh & Bothun 1994). It is possible to use the correlation properties of the extragalactic background to constrain galaxy evolution models (Cole, Treyer & Silk 1992). However, this type of analysis must take into account that a significant fraction of the background from discrete sources is at much lower redshifts than the galaxies seen in deep pencil beam surveys, and that LSB galaxies are more readily detected in pencil beam surveys than in wide field surveys.

GAS MASS DENSITY Galaxy evolution proceeds by the conversion of gas into stars. There is ample evidence that the census of diffuse galaxies as measured by their light is incomplete. However, the search for gas through the 21 cm emission line offers a complementary approach. Radio telescopes have been used not only to measure the gas contents of cataloged galaxies, but to place limits on the space density of intergalactic clouds of neutral hydrogen (Fisher & Tully 1977). For a source larger than the beam,

$$(N_{\rm HI})_{\rm lim} > 2 \times 10^{16}\ (S/N)\ T_{\rm sys} \left(\frac{\Delta V}{t}\right)^{1/2} {\rm\ atoms\ cm^{-2}} \quad (11)$$

where t is the integration time, ΔV in kms^{-1} is the bandwidth in terms of the antenna equation or the velocity dispersion of the gas for a galaxy, and $(N_{\rm HI})_{\rm lim}$ is independent of telescope size because telescope area and beam size cancel (Disney & Banks 1997). For sources smaller than the beam, the visibility volume is given by

$$V(M_{\rm HI}, \Delta V) \propto n_{\rm beam} D t^{-1/4} \left(\frac{M_{\rm HI}}{\sqrt{\Delta V}} \right) \quad (12)$$

where t is the integration time per pointing or beam, which means that the typical observing strategy is to maximize the observable volume with short integrations and a shallow survey. As a consequence, very little is known about the HI content below a column density of $N_{\rm HI} \sim 10^{19}$ atoms cm^{-2}. There is a rough scaling $N_{\rm HI} \sim 10^{20} (M_{\rm HI} / L_{\rm B}) 10^{0.4(27 - \mu_{\rm B})}$ *atoms cm*$^{-2}$ (Disney & Banks 1997), such that galaxies from most HI surveys should be readily detectable on POSS II or UKST survey plates, and galaxies with either $N_{\rm HI} < 10^{19}$ atoms cm^{-2} or $\mu_e > 27$ mag arcsec^{-2} are extremely difficult to detect by any technique.

Published radio surveys have a number of limitations. The sensitivity to HI masses below 10^8 $M_\odot$ is poor, and the small beam sizes and limited bandwidths allow relatively small volumes to be probed, with correspondingly weak limits on rare objects. Interferometers gain over single dishes by the number of beams per field of view, but lose bandwidth due to the need for $n(n - 1)$ correlators, where n is the number of telescopes in the array. Equally important is the region of space targeted. Most surveys have targeted optically-selected galaxies, which involves a bias towards those galaxies that have been most efficient in forming stars. Other surveys target optically bright galaxies, but are sensitive to HI signals elsewhere in the velocity bandwidth, or in the "off" beams. This prejudices the sample to the immediate environments of bright galaxies, which may be atypical. Many HI surveys are confined to the Local Supercluster, a volume which is overdense by a factor of ~ 2.3 compared to the cosmic average (Felten 1977). There have been relatively few unbiased HI surveys.

Schneider et al (1990, 1992) have published extensive HI surveys, including observations of many dwarf and LSB galaxies (mostly from the UGC catalog). Rao & Briggs (1993) have calculated the HI mass function of late-type galaxies over the range $10^7 < M_{\rm HI} < 10^{10}$ $M_\odot$ using the surveys of Fisher & Tully (1981) and Hoffman et al (1989). Other "blind" surveys have been used to quantify the space density of gas-rich dwarfs (Weinberg et al 1991, Szomoru et al 1994) and giants (Briggs 1990). The HI mass function has an analogous form to the Schechter luminosity function

$$\Theta(M_{\rm HI}) d(M_{\rm HI}) = \left(\frac{\phi^*}{\beta + 1} \right) \left(\frac{M_{\rm HI}}{M^*_{\rm HI}} \right)^{\frac{-(\alpha+\beta)}{(1+\beta)}} \exp \left(\frac{-M_{\rm HI}}{M^*_{\rm HI}} \right)^{\frac{1}{(1+\beta)}} d \left(\frac{M_{\rm HI}}{M^*_{\rm HI}} \right) \quad (13)$$

where the extra component is the trend of HI richness with luminosity $M_{\rm HI} / L \propto L^{\beta}$. Studies of spiral and irregular galaxies indicate $\beta \approx -0.1$ (Fisher & Tully 1975), and when β is small the shape of the HI mass function and the optical luminosity function are very similar (Rao & Briggs 1993). Figure 4a shows a direct comparison between the Rao & Briggs mass function and the count of LSB galaxies from the APM survey, normalized at $M_{\rm B} = -21$ or $M_{\rm HI} = 3 \times 10^9$ $M_\odot$. Both functions are consistent with a faint end slope corresponding to $\alpha = -1.4$ in a Schechter parametrization.

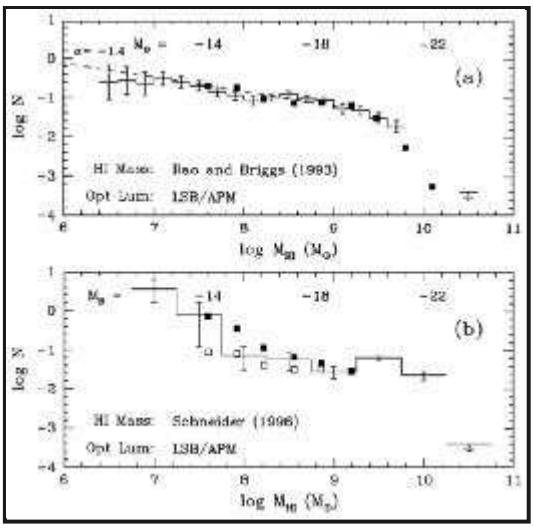

Figure 4. (a) The HI mass function and the LSB galaxy number distribution superimposed, using the mean realationship between light and gas mass from the APM LSB survey, normalized at M_B = -21. (From Rao & Briggs 1993, Impey et al 1996, Sprayberry et al 1997). (b) As above, with the HI mass function taken from a deep Arecibo survey. The open squares are the APM counts of LSB galaxies as in (a), the filled squares show the counts using a correction for censored regions in the surface brightness-luminosity plane. (Sources as above, in both cases the limit on high HI mass Malin 1-type galaxies is from Briggs 1990.)

Figure 4b shows the mass function from a sensitive Arecibo HI survey (Schneider 1996), with the luminosity function of the LSB galaxies from the APM survey superimposed. Optical luminosity is mapped onto HI mass for the APM sample by the relation $M_{HI} = 10^{10 - (M_B + a)/b} M_\odot$, with a = 21.7 and b = 3.16, which accounts for the fact that the galaxies are optically selected, and so the distribution is censored at low values of M_{HI} for a given luminosity. This relationship agrees well with the slope (to 10%) and the normalization at $10^8 M_\odot$ (to 50%) of the relationships adopted by Briggs (1990), a = 20.3 and b = 2.78, and Tyson & Scalo (1988), a = 20.9 and b = 3.12. LSB galaxies are a factor of ~ 2 more gas-rich at a given luminosity than HSB galaxies. The two functions are normalized at $M_{HI} = 3 \times 10^9 M_\odot$ where the HI survey is reasonably complete.

The HI mass function shows a clear upturn at $M_{HI} \sim 10^8 M_\odot$, corresponding to $M_B \sim$ - 16, where the APM luminosity function turns up with a faint end slope of α = - 1.4. At the high end of the HI mass function, Briggs (1990) has put a limit on the space density of giant gas disks like Malin 1 (also see Bothun 1985). With 95% confidence assuming Poisson statistics, $\rho < 4.1 \times 10^{-4}$ Mpc^{-3} (Weinberg et al 1991 have a weaker limit of $\rho < 0.029$ Mpc^{-3}). This upper bound is weak enough that objects like Malin 1 could contribute as much integrated gas density as HI rich dwarfs with $M_{HI} = 10^8 M_\odot$. Several thousand such galaxies could lie closer than the prototype. Nevertheless, the cosmological conclusion is that gas-rich LSB galaxies do not domnate the local gas mass density of the universe.

MASS DENSITY IN BARYONS Even after correcting for surface brightness selection, the luminosity density is one step removed from the function of cosmological interest. The baryonic density is

$$\rho_{\rm baryon} = \sum \int \phi(L,\mu)\Gamma(L,\mu) L dL d\mu \quad (14)$$

where both the luminosity function and the baryonic mass-to-light ratio $\Gamma(L, \mu) = (M / L)_{\rm baryon} = A(\mu)(L / L_*)^\eta$ are functions of surface brightness. A large amount of uncertainty is hidden in the normalization factor $A(\mu)$, because there is very little data on the dependence of baryonic M/L as a function of surface brightness. To simplify, we can factor A out of the integral

$$\rho_{\rm baryon} = \phi^* L^* A \int_{L_{\rm min}}^{L_{\rm max}} (L/L^*)^{1+\alpha+\eta} \exp(-L/L^*) d(L/L^*) \quad (15)$$

where the surface brightness corrections to the luminosity function are accounted for in terms of an increased normalization, ϕ^*, and a steeper faint end slope, α. Following Persic & Salucci (1992), we take the bounds of the integral as $0.01 < (L / L^*) < 8$. Bristow & Phillipps (1994) plot the integrated mass function for different values of α, η, and $L_{\rm min}$.

To sharpen up the cosmological comparison, we use recent nucleosynthesis constraints (Copi, Schramm & Turner 1995), and a Hubble constant bound of $0.5 < h_{100} < 0.8$ which encompasses 95% of the published values since 1995 (Kennicutt, private communication), including the recent HST Key Project result of $H_0 = 73 \pm 10$ kms^{-1} Mpc^{-1} (Freedman, Madore & Kennicutt 1997). Although we use a scaling to $H_0 = 100$ km s^{-1} Mpc^{-1} in this review, it is almost certain that $h_{100} < 1$, and a number of direct distance scale measurements indicate $h_{100} < 0.7$ (e.g. Saha et al 1996, Grogin & Narayan 1996). The result is $0.014 < \Omega_{\rm baryon} < 0.080$, which may increase by a factor of 2-3 if the D/H ratio proves to be as low as 1-2 $\times$ 10^{-5}. Most matter is nonbaryonic, and most baryons have not yet been detected.

Given the uncertainties in this calculation, we quote only illustrative results. For spirals, Persic & Salucci (1990) derive $A = 2.4h_{100}(M_\odot / L_\odot)$, whereas McGaugh (1992) derives $A \approx 5h_{100}(M_\odot / L_\odot)$ for LSB spirals, a ratio of a factor of 2.1. Based on the APM survey (Impey et al 1996), we increase the normalization by a factor of 1.3. The product of these two factors raises the spiral contribution by a factor of 2.7, and the overall Persic & Salucci census by 40% to $\Omega_{\rm baryon} = 0.0042$. The biggest leverage in the mass density integral comes from faint and low mass galaxies. Persic & Salucci (1990) assume values which make the exponent $1 + \alpha + \eta > 0$, but if $1 + \alpha + \eta < -1$ the mass integral rises rapidly. Adopting a faint end slope of $\alpha = -1.4$, and assuming $\eta \approx 0$ (because LSB galaxies appear to have higher M / L and since luminosity and surface brightness are correlated), $\Omega_{\rm baryon} = 0.0062$. If either $\alpha = -1.80$, or $\eta = -0.5$ (baryons scale with dark matter), the correction factor becomes 3.6, with a total $\Omega_{\rm baryon} = 0.013$. Bristow & Phillipps (1994) use more extreme, but not implausible, values to deduce $\Omega_{\rm baryon} = 0.025$. We conclude that LSB galaxies can easily be the sites of much of the "missing" baryonic matter in the universe.

TOTAL MASS TO LIGHT RATIOS Dynamical measures of the total mass-to-light ratios of LSB galaxies are difficult to obtain. A small number of HI rotation curves of LSB giants have been published (de Blok, McGaugh, & van der Hulst 1996), but velocity dispersions for the LSB dwarfs are beyond the capabilities of existing telescopes. There is nonetheless indirect evidence that LSB galaxies have higher M / L than HSB galaxies of the same size. It has been found that LSB disks follow the same Fisher-Tully relation as normal bright spirals, but with increased scatter (Zwaan et al 1995, Sprayberry et al 1995b). If the mass M is proportional to $v_{\rm max}{}^2 h$, then $v_{\rm max}{}^4 \propto M^2 / h^2 \propto M^2 I_0 / L$, since $L \propto I_0 h^2$. Zwaan et al (1995) found that LSB galaxies from the surveys of McGaugh & Bothun (1994), Knezek (1993), and de Blok, van der Hulst & Bothun (1995) have the same luminosities at a fixed line width as the HSB galaxies observed by Broeils (1992). This implies $M / L \propto I_0{}^{-1/2}$. Although the scatter is large, luminosity and central surface brightness are correlated for the APM sample, with a dependence that scales as $L \propto I_0{}^{1/2}$. Using a projection of the luminosity-surface brightness distribution that accounts for censored galaxies, this flattens to $L \propto I_0$. With this latter dependence $M / L \propto L^{-1/2}$, which gives LSB galaxies considerable leverage in the mass census of disk systems.

Less can be said about the M / L of dwarf LSB galaxies in the field, because the galaxies are small and the HI line widths are narrow (10-30 km s^{-1}), so the rotation curves are usually poorly sampled. The low surface mass density of the (mostly gas-poor) LSB dwarfs in clusters like Virgo and Fornax suggests a stability constraint. Assuming isotropic velocities, the mass density in the core of a rich cluster is

$$\rho_c = \frac{9\sigma^2}{4\pi G r_c^2} = 3 \times 10^{-3} h_{100}^2 \ M_\odot {\rm pc}^3 \quad (16)$$

where $\sigma = 870$ kms^{-1} and $r_c = 0.2h_{100}{}^{-1}$ Mpc (Peebles 1993). This number can be compared with the stellar mass density of a typical LSB galaxy

$$\rho_{\rm LSB} = \frac{L(r)}{V(r)}(M/L)_{\rm LSB} = 3\left[\frac{L_{\rm tot}\{1-(1+n)e^{-n}\}}{4\epsilon\pi(nh)^3}\right](M/L)_{\rm LSB} \quad (17)$$

where n is the number of scale lengths considered, and ϵ is a shape parameter that describes the departure from spherical symmetry. Adopting $n = 3$ (which includes 80% of the total light) and $\epsilon = 0.3$ leads to a condition for the stability of the diffuse galaxy in the tidal field of a cluster core $(M / L)_{\rm LSB} > 0.13(h^3 / L_{\rm tot})$, where h is in parsecs and $L_{\rm tot}$ is in solar units. The envelope of this distribution is of course defined by selection effects, which mitigate against the combination of large scale length and low luminosity. However, cluster LSB samples (Impey, Bothun & Malin 1988; Bothun, Impey, & Malin 1991; Turner et al. 1993) include galaxies whose long term existence implies larger than expected mass-to-light ratios. The condition $M / L > 3$ corresponds to $h > 3$ kpc at $M_{\rm B} = -17$ or $h > 10$ kpc at $M_{\rm B} = -21$. Finally, we note that the innocuous Local Group dwarf spheroidals have some of the highest M / L ratios of any galaxies (Mateo 1996). The galaxies that have been undercounted in all existing surveys are those with the highest mass fractions of gas and the the highest M / L ratios.

4.2. Galaxy Evolution

Our understanding of how galaxies form and evolve is highly incomplete. Ironically, we know as much about the linear and high temperature physics during the first few minutes of the universe, through the successes of the hot big bang model (e.g. Peebles et al 1991), as we do about the billion years after density perturbations became nonlinear. Our ignorance of galaxy evolution has hampered tests of the deceleration parameter and the curvature of the universe (Sandage 1988). Reliable measures of ages and stellar populations can only be obtained for nearby, prominent galaxies. These same high surface brightness galaxies are used as probes of large scale structure in redshift surveys. The study of low surface brightness galaxies opens a new window onto galaxy formation and evolution.

THE COLORS OF LSB GALAXIES The LSB dwarf galaxies in clusters are distinguished by their blue colors and low gas contents. Imaging of sufficient resolution reveals mostly dIm and dE morphologies. In Virgo and Fornax combined, the mean colors are $B - V = 0.58 \pm 0.02$ for 31 objects, and $V - I = 1.00 \pm 0.03$ for 23 objects (Impey, Bothun, & Malin 1988; Bothun, Impey, & Malin 1991). Davies, Phillipps, & Disney (1990) found $B - R \approx 1.4$ in Fornax, corresponding to a slightly redder $B - V \approx 0.7$. There is no simple explanation for these colors, which are similar to the colors of the most metal-poor galactic globular clusters. The lack of a correlation between color and surface brightness argues against LSB dwarfs being faded remnants of more gas-rich dwarfs. One scenario identifies the diffuse stellar component as a fossilized metal-poor remnant of a galaxy with a steadily softening potential, where most of the gas was driven away long ago (Dekel & Silk 1986). Although the blue colors are consistent with a young median age, spectroscopy is required to disentangle effects of age and metallicity.

Although fading is not indicated as a cause for the low surface brightness, a red population of LSB galaxies cannot be ruled out. All of the large area surveys have been carried out in the blue, and a star-bursting dwarf could rapidly redden and fade below threshold imposed by the night sky. A 10^7 year starburst with a conventional IMF would redden from $B - V = -0.30$ to $B - V = 0.50$ after 10^9 years, whereas the total light fades by ~ 5 magnitudes (Bruzual & Charlot 1993). After 10^{10} years, the color reddens further to $B - V = 0.85$ and the total light fades another ~ 2 magnitudes. Assuming the galaxy fades with constant scale length, a galaxy fading by $\Delta\mu$ magnitudes is lost more rapidly due to falling below the angular size limit ($n \propto \Delta\mu^3$) than it is due to falling below the flux limit ($n \propto 10^{\Delta\mu / 2.5}$). Each factor of two of fading reduces the visibility volume by a factor of eight. In addition, the sky contrast improves towards the blue for all objects with $B - I < 1.3$. The combined result is a formidable selection effect against post-starburst LSB dwarfs.

LSB disk galaxies also have blue colors. After excluding galaxies with significant bulges, McGaugh & Bothun (1994) found $U - B = -0.17$, $B - V = 0.49 \pm 0.04$, and $V - I = 0.89$, similar to the colors of an actively star-forming Sc galaxy. Romanishin, Strom, & Strom (1983) found averages of $B - V = 0.43 \pm 0.04$ and $V - R = 0.60 \pm 0.02$. This compares with $B - V = 0.75 \pm 0.03$ and $V - R = 0.53$ for normal spirals that are on average 2 magnitudes brighter in $\mu_{\rm B}$ (de Jong & van der Kruit 1994). For seven giant LSB disks, Sprayberry et al. (1995a) found $B - V = 0.73 \pm 0.05$ and $V - R = 0.50 \pm 0.04$. LSB galaxies in general are about 0.25 magnitudes bluer in $B - V$ than HSB galaxies, and both populations show a correlation between increasing redness and larger scale length. This effect, plus the fact that there is no correlation between color and surface brightness, can be used to rule out fading as a cause of the low surface brightness for both LSB giants and dwarfs. The HII region oxygen abundances are also uncorrelated with color, which means that the blue colors are not caused by low metallicity. Metallicities are typically 1/3 solar (McGaugh 1994a).

Sprayberry et al (1995a) found four Seyfert 1 nuclei and one Seyfert 2 nuclei in a study of 10 LSB giants, as indicated by broad Hα emission and sometimes [NII] / Hα ratios indicative of excitation by a power law (see also Knezek 1993). Although the sample is small, the Poisson probability of drawing so many Seyferts from a population of normal galaxies with the same luminosity (Meurs & Wilson 1984) is small, $\sim 2 \times 10^{-6}$. It is possible that the kinematics of a low surface mass density disk can

facilitate mass transfer into the central parsec, where it can fuel nuclear activity.

GAS CONTENT AND EVOLUTION Combining radio and optical data leads to a better understanding of the evolution of LSB galaxies. The HI properties of LSB galaxies as a class were first studied by Hawarden et al (1981). More recently, radio synthesis telescopes have been used to derive rotation curves and to map out the gas in the disk. LSB disks have low star formation rates, despite their normal HI contents and luminosities. Kennicutt (1989) has shown that the star formation rate in HSB disks has a threshold, below which widespread star formation does not occur. The critical HI surface mass density is

$$\Sigma_{\rm crit} = \frac{\eta \sigma_v V}{2.38 G R} \left(1 + \frac{R}{V}\frac{dV}{dR}\right)^{1/2} \qquad (18)$$

where η is a dimensionless constant around unity, σ_v is the velocity dispersion in the gas disk, and the circular velocity of the gas is V at radius R. Using HI synthesis data from the Westerbork Telescope, van der Hulst et al (1993) have found that LSB disks have HI surface mass densities of 3-6 $M_\odot$ pc^{-2}, a factor of two lower than HSB disks (Cayette, Kotanyi, & Balkowski 1993). This puts most of the disk below the threshold for star formation, given by $\Sigma_{\rm crit} = 0.059\, \sigma_v (V / R)\, M_\odot pc^{-2}$, where σ_v is in kms^{-1}, and where V is the rotation velocity in kms^{-1} at a distance R in kpc.

The physical basis for this threshold is the onset of gravitational instability in a thin, rotating disk (Toomre 1964, Quirk 1972). Star formation is therefore governed by local physics; despite the low overall rate, the star formation in isolated regions can be prodigious (Impey & Bothun 1989). A plausible hypothesis is that the evolution of all galaxies is driven by surface mass density. Since mass is roughly given by $M \propto v_{\rm max}{}^2 h$, and since both HSB and LSB galaxies follow a Fisher-Tully relation, $L \propto v_{\rm max}{}^4$, it follows that $(M / L) \propto v_{\rm max}{}^2 h / (Mh)^2 \propto \bar{\Sigma}$, where $\bar{\Sigma}$ is the mean surface mass density (de Blok, van der Hulst & Bothun 1995). Low surface mass density galaxies evolve slowly, forming few stars, which results in low surface brightness and high values of M / L.

It is important to reiterate the facility with which quiescent and low mass galaxies can escape detection by either optical or radio surveys. The neutral disks of spiral galaxies are observed to truncate sharply below a column density of 2-3 $\times$ 10^{19} atoms cm^{-3} (e.g. van Gorkom et al 1997). As the column density of HI falls off, galaxy disks can be ionized, which rapidly reduces the detectable HI mass (Maloney 1993, Corbelli & Salpeter 1993, Dove & Shull 1994). As parametrized by Dalcanton, Spergel, & Summers (1997a), the observable HI mass is $M_{\rm HI} = 50\pi \Sigma_{\rm HI} h^2 [1 - 0.01 \Sigma_{\rm HI}{}^{-1.43} (5.61 + 1.43 \ln \Sigma)]\, M_\odot$, where h is in units of kpc and $\Sigma_{\rm HI}$ is in units of 10^{21} atoms cm^{-2}. This trend is illustrated in the left panel of Figure 5. Galaxies with scale lengths under 5 kpc or central surface HI densities under 10^{20} atoms cm^{-2} drop below the sensitivity limit of a typical Arecibo survey. Galaxies with scale lengths under 2 kpc or central surface HI densities under 3 $\times$ 10^{19} atoms cm^{-2} are difficult to detect in any HI survey.

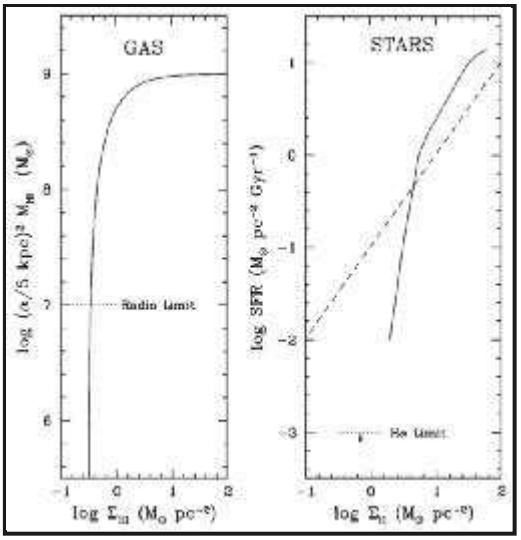

Figure 5. The left hand panel shows the detectivity of HI as a function of scale length and surface mass density of gas. (From Dalcanton, Spergel & Summers 1997a.) The right panel shos the dependence of disk star formation rate on the surface mass density of gas, HI plus H_2. The dashed line corresponds to a constant star formation rate over a Hubble time. (From Kennicutt 1989.)

There is a similarly rapid drop in the detectability of newly formed stars as a function of the total (HI plus H_2) hydrogen surface density. Using a conversion from Hα flux to star formation rate from Kennicutt (1983), the dependence of Hα surfac brightness on total hydrogen surface density for Sc galaxies (Kennicutt 1989) can be parametrized in a quasi-Schechter form as $\Sigma_{SFR} = 2.72 \exp(-5/\Sigma_H)(-5/\Sigma_H^{-0.78})\ M_\odot\ pc^{-2}\ Gyr^{-1}$, where Σ_H is in units of $M_\odot$ pc^{-2}. Note that this is only a rough scaling, as the threshold surface densities range from 2-10 $M_\odot$ pc^{-2}, and the Hα surface brightness at a given hydrogen surface density ranges over more than a factor of ten. The right panel of Figure 5 shows this dependence, where the dashed line represents a steady star formation rate over a Hubble time. Below a few $M_\odot$ pc^{-2}, the star formation rate drops so low that Hα emission is no detectable, and the rate of gas consumption is so low that the galaxy is essentially quiescent.

4.3. Implications for Quasar Absorption

The narrow absorption lines seen in the spectra of quasars are powerful probes of dim and low column density material along the line of sight. The neutral hydrogen column densities of the absorbers range over ten orders of magnitude, $10^{12} < n_{HI} < 10^{22}$ cm^{-2}. The high column density or "damped" Lyman-α systems have associated metals, and may be the progenitors of normal spiral galaxies. The low column density systems of the Lyman-α "forest" have much lower metallicity, and are only weakly associated with galaxies. Intermediate HI column densities are probed by the CIV $\lambda\lambda$1548,1550 and MgII $\lambda\lambda$2797,280 absorption doublets, which are strongly clustered in velocity space, and are presumed to originate in the halos of normal galaxies, which are sometimes located in clusters. For a recent review, see the proceedings edited by Meylan (1995).

The number of absorbers per unit redshift down to a particular rest equivalent width line is given by

$$\frac{dN}{dz} = \frac{c\sigma n}{H_0}(1+z)^\gamma (1-q_0 z)^{-1/2} \int_0^\infty \phi_g(L) A(L) dl \quad (19)$$

where $\Phi_g(L)$ is the conventional Schechter function multiplied by f_g, the fraction of gas-rich galaxies, basically spirals and irregulars. We assume no evolution in the redshift path density, i.e. $\gamma = 1$, which is appropriate for both the MgII absorbers (Steidel & Sargent 1992), and for the low column density Lyman-α absorbers at low redshift (Bahcall et al 1993). It is also likely to be appropriate for the high column density, damped Lyman-α absorbers (Lanzetta et al. 1991, but see Rao, Turnshek & Briggs 1995). The cross sectional area of the absorbers is $A(L/L^*) = (\pi R_*^2/2)(L/L^*)^{2\beta} \eta^2$, where R_* is a fiducial radius.

typically the Holmberg radius for an L^* galaxy, and η is a factor that relates the optical size of a galaxy to the HI size at the column density of interest. This yields

$$\frac{dN}{dz} = \left(\frac{\pi c}{2H_0}\right)(\eta R_*)^2(f_g\phi^*)(1+z)(1-q_0 z)^{-1/2}\Gamma(1+2\beta+\alpha) \quad (20)$$

The absorption path length depends on the galaxy luminosity, the faint end slope of the luminosity function, and the relationship between absorption cross-section and luminosity. Assuming no evolution of the galaxy luminosity function (either Φ^* or α) over the path length, the integral over redshift gives the fraction of the absorption path length that is caused by galaxies brighter than a certain luminosity. The conventional Holmberg (1975) relation is $(R / R_*) \propto (L / L^*)^{0.4}$. Using this scaling and the conventional $\alpha = -1$, dwarfs with $M_B > -16$ should contribute ~ 10% of the absorption cross section.

METAL LINE ABSORBERS MgII absorbers are equivalent to absorbers selected to be optically thick in the Lyman continuum, $\tau(912\ \text{Å}) > 1$ or $N_{HI} > 3 \times 10^{17}$ atoms cm^{-2} (Sargent, Boksenberg & Steidel 1988). There is strong statistical evidence linking MgII absorption to the presence of a bright galaxy near the line of sight (Bergeron & Boisse 1991, Steidel & Dickinson 1992). The traditional Holmberg scaling is almost certainly not appropriate. Impey, Bothun, & Malin (1988) showed that for a Virgo sample of galaxies all at roughly the same distance, the relation $R \propto L^{0.4}$ is partly a consequence of selection effects caused by sky brightness. Steidel (1993) studied the impact parameters of galaxies causing 56 MgII absorptions over the range $0.2 < z < 2.2$. The results were inconsistent with $\beta = 0.4$, and had a maximum liklihood fit of $\beta = 0.2$ and $R_* = 35 h_{100}^{-1}$ kpc. The scaling $R \propto L^{0.2}$ with $\alpha = -1$ implies that dwarfs contribute ~ 75% of the absorption cross section. Alternatively, we can adopt $\beta = 0.4$, and consider the effect of a steep faint end slope to the luminosity function. Dwarfs contribute 35% of the cross section if $\beta = 0.4$ and $\alpha = -1.4$, and 85% of the cross section if $\beta = 0.4$ and $\alpha = -1.7$. The integral $\int \Phi(L) A(L)\, dL$ diverges and dwarfs dominate the cross section for any combination $\alpha + 2\beta \leq -1$.

Equation (20) uses local galaxy properties to predict the demographics of the quasar absorbers. This can be compared with the observed properties of individual absorbers, which are detected as galaxies with the appropriate redshift lying at small impact parameters from the quasar sightline. Steidel (1993) found no absorbers with $M_B > -19.4 + 5 \log h_{100}$, as opposed to 80% predicted if $\beta = 0.2$, and 50% predicted if $\alpha = -1.4$. This sharp difference implies that copious gas-rich dwarfs (York et al 1986, Tyson & Scalo 1988) or unseen low surface brightness galaxies (Phillipps, Disney & Davies 1993) cannot be a major contributor to Mg II absorption. We also consider it unlikely that f_g declines with decreasing luminosity; a number of field galaxy luminosity functions have a rising tail of primarily gas-rich dwarfs. However, the gas in low mass galaxies is probably ionized, so that dwarfs are not responsible for HI absorption in the range $3 \times 10^{17} < N_{HI} < 3 \times 10^{19}$ atoms cm^{-2}. Maloney (1993) has shown that the column density N_{crit} below which gas is ionized, and therefore galaxies are mostly invisible in the 21 cm line, is a function of halo surface mass density, $N_{crit} \propto \Sigma_{halo}^{0.6}$. Low mass or low surface mass density galaxies will therefore be ionized at larger total gas column densities.

HIGH COLUMN DENSITY HYDROGEN ABSORBERS The most massive gas disks produce damped Lyman-α absorption with HI columns in the range $2 \times 10^{20} < N_{HI} < 6 \times 10^{22}$ atoms cm^{-2}. At a mean redshift of $z = 2.5$, the absorbers have $dN/dz \approx 0.2$ and contribute $\Omega = 1.45 \times 10^{-3}\ h_{100}^{-1}$ ($q_0 = 0.5$) to the mass density of the universe (Lanzetta et al 1991). Impey & Bothun (1989) made the point that gas-rich LSB disks have many similar properties to the progenitors of spiral galaxies seen at high redshift, including size, HI column density, and a low mean star formation rate. Bergeron (1995) has directly observed LSB galaxy counterparts to damped Lyman-α absorbers at intermediate redshift.

For the large LSB disks, the observational bounds are $2.8 \times 10^{-5} < dN / dz < 1.9 \times 10^{-2}$. The upper bound comes from the diameter, $140 h_{100}^{-1}$ kpc at the 3×10^{19} atoms cm^{-2} contour, and the limit on the space density of less than 4.1×10^{-4} Mpc^{-3} for objects like Malin 1. The much less restrictive lower bound comes from the minimum space density of galaxies in the tail of the size distribution of UGC galaxies, those with diameter greater than 50 kpc. Rao & Briggs (1993) derived $dN/dz = 0.015 \pm 0.004$ for the gas cross section of normal galaxies at the present epoch, so it is possible than giant disks like Malin 1 are the largest contributor to high column density HI absorption. The upper bound on the incidence of damped Lyman-α systems at low redshift is $dN/dz < 0.05$ (Storrie-Lombardi et al 1994). The contribution of damped Lyman-α systems to the density parameter at $z \sim 0$ is found to be $\Omega = 1.9 \times 10^{-4}$ (Lanzetta, Wolfe, & Turnshek 1995). This can be compared to the bounds from the gas and stars in giant LSB galaxies: $\Omega_{gas} = \rho_{gas} / \rho_{crit} < 1.5 \times 10^{-4}$, where $\rho_{crit} = 2.78 \times 10^{11}\ h_{100}^2\ M_\odot$ Mpc^{-3}, and an HI mass of $10^{11}\ M_\odot$ is adopted for Malin 1, and $\Omega_{stars} = \rho_{stars} / \rho_{crit} > 1.1 \times 10^{-4} (M / L)$, where we use the luminosity density of LSB galaxies, 3 ± 0.5

$\times 10^7 h_{100}\ L_\odot\ Mpc^{-3}$. Therefore, large gas disks can be a substantial contributor to the local population of damped Lyman-α absorbers.

LOW COLUMN DENSITY HYDROGEN ABSORBERS The last comparison concerns the low HI column density absorbers of the Lyman-α forest, which have $dN/dz \approx 100$ for $N_{HI} > 10^{13}$ atoms cm^{-2} (Morris et al 1991), and $dN/dz \approx 15$ for $N_{HI} > 10^{14}$ atoms cm^{-2} (Bahcall et al 1993). Tyson (1988b) speculated that the copious low column density absorbers were associated with gas-rich dwarf galaxies. The space density of the absorbers is $\rho = 2.9 \times 10^{-2}\ Mpc^{-3}$, where we adopt the large characteristic absorber size of $500 h_{100}^{-1}$ kpc at $z \sim 0.7$, measured by Dinshaw et al (1995) using common absorption in a quasar pair to define a size. The maximum liklihood technique yields a 95% confidence interval which translates to $\rho_{Ly\alpha} = 0.3\text{-}3.7 \times 10^{-2}$ Mpc^{-3}. This overlaps with the observational range of the number density of low luminosity galaxies $N_{gal} = 1.1\text{-}6.3 \times 10^{-2}\ Mpc^{-3}$, which makes use of the density of $M_B = -14$ galaxies from Loveday et al (1992) as a lower bound, and using the surface brightness corrected density of $M_B < -14$ galaxies from the APM LSB survey as an upper bound.

LSB galaxies share the space density and clustering properties of Lyman-α absorbers seen at somewhat higher redshifts. Rauch & Haehnelt (1995) showed that for uniform clouds of thickness D and temperature T in a UV ionizing background I (in units of 10^{-21} erg Hz^{-1} sr^{-1} s^{-1} cm^{-2}), $\Omega_{baryon} \approx 0.027 h_{100}^{-1}\ (T/3 \times 10^4\ K)^{1/3}\ I^{1/2}\ (D/100\ kpc)^{1/2}$. If the clouds are large and elongated, most baryons may be in this form. Direct association of low redshift absorbers with LSB galaxies is unlikely; it has been ruled out in some cases (Rauch, Weymann & Morris 1996). On the other hand, the association of the absorbers with bright galaxies is difficult to prove; all that the observations provide is an impact parameter, and there may be undetected galaxies closer to the line of sight. Large samples are required before the kinematics and peculiar velocities of the absorbers can be compared with similar information for the galaxies along the line of sight. Simulations which incorporate gas dynamics have shed some light on the situation. The low column density HI absorbers form a filamentary network that traces out the dark matter potential of large scale structure (Cen et al 1994, Petitjean, Mucket & Kates 1995, Hernquist et al 1996). The copious number of observed LSB dwarfs might be associated with collapsed regions within a more extensive network of diffuse hydrogen.

4.4. Galaxy Formation

LSB GALAXIES AT COSMOLOGICAL DISTANCES The discussion so far has concentrated on the properties of LSB galaxies in the local universe. However, these unassuming stellar systems have great relevance for surveys of galaxies at cosmological distances and significant lookback times.

The visibility of galaxies is defined by the isophotal limits of the survey, but it is also a strong function of galaxy redshift and type. As first discussed by Phillipps, Davies & Disney (1990), galaxies in deep surveys are more likely to be blue and of high surface brightness, since those types have a large accesible volume. The cosmological corrections give

$$(\mu_{\rm lim} - \mu_0)_{\rm obs} = (\mu_{\rm lim} - \mu_0)_{z=0} - 10\log(1+z) - k(z) \quad (21)$$

and

$$M_B = m_B - 5\log\{(2c/H_0)(1+z)(1-(1+z)^{-1/2})\} - 25 - k(z) \quad (21)$$

where $k(z)$ are the k-corrections. As we consider galaxies at higher and higher redshifts, the visibility is reduced by a combination of k-corrections and the Tolman $(1+z)^4$ cosmological dimming of the surface brightness (Phillipps, Davies & Disney 1990). Figure 6 shows the visibility distance for spirals (panel a) and ellipticals (panel b), assuming an angular diameter limited survey with three different values of θ_{lim} plotted. The dashed curves show the selection functions with cosmological effects (k-corrections, Tolman surface brightness dimming) included. The peak visibility of ellipticals at zero redshift is 30% smaller than that of spirals, and ellipticals have larger k-corrections. The result is that ellipticals are much less visible than spirals in deep optical surveys.

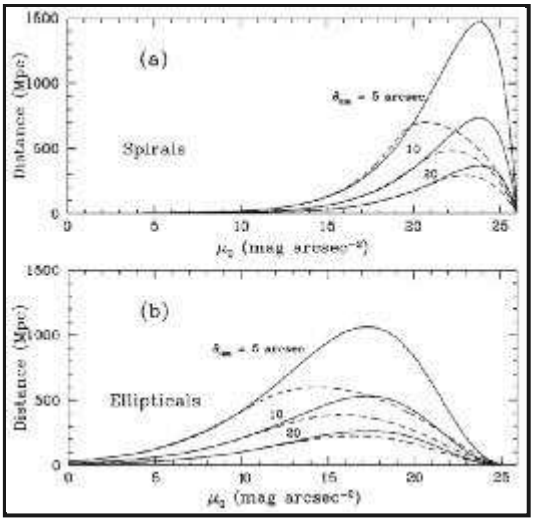

Figure 6. (a) The visibility distance for spirals assuming three different values of the angular size limit in arcseconds. The dashed curves show the effect of cosmological corrections to the visibility distance. (b) As above, for elliptical galaxies. In both cases, M_B = - 21 has been assumed, the curves for other cases scale with the luminosity distance. (From Phillipps, Davies & Disney 1990.)

The isophotal limits of the pencil beam CCD surveys are so deep that those surveys are sensitive to galaxies that are absent from local, wide field surveys. The curves superimposed on Figure 2 illustrate this important point (see also McGaugh 1994b). The far left solid curve shows the selection function of the APM LSB survey (Sprayberry, Impey & Irwin 1996), assuming μ_{lim} = 26 B mag arcsec^{-2} and θ_{lim} = 10 arcsec. The two curves to the right show the equivalent selection function at z = 0.1 and z = 0.5. Only the most luminous and high surface brightness galaxies at z = 0.5 are detected on Schmidt photographic plates. Whereas about 30% of RC3 galaxies fit this criterion, only about 10% of the APM sample do. The dashed curve shows the selection function at z = 0.5 for the deep CCD survey of Lilly (1993), with limits of μ_{lim} = 28.6 B mag arcsec^{-2} and θ_{lim} = 2 arcsec. The CCD survey encompasses a larger region of (μ,L) space at z = 0.5 than the APM survey does in the local universe. In other words, deep CCD surveys are sensitive to a potentially large number of galaxies (not neccesarily dwarfs) that are essentially absent from published wide field surveys.

RELATION TO DEEP GALAXY SURVEYS The number of faint galaxies in the B and I bands exceeds the expectations of all cosmological models that do not include evolution (Tyson & Jarvis 1979, Kron 1982, Tyson 1988a, Lilly, Cowie & Gardner 1991). The excess of blue galaxies must however be reconciled with the observed redshift distribution at B = 24, which is consistent with a no evolution prediction. Many of the solutions that have been proposed so far are problematical. The excess population at z = 0.3-0.5 cannot be removed by merging because the faint blue galaxies are not strongly enough clustered (Efstathiou et al 1991), and the requisite merger remnants cannot be found (Dalcanton 1993). Selective luminosity evolution has also been proposed, where a high space density of bright dwarfs evolves strongly to become a common but faint population locally (Broadhurst, Ellis & Shanks 1988, Lilly 1993). This rapid and strong evolution has not been observed to occur. The distasteful option of a cosmological constant has probably been ruled out by the statistics of gravitational lensing (Fukagita & Turner 1991). More conservative solutions involve adjustments of the local luminosity functions of the different galaxy types (Koo, Gronwall & Bruzual 1993). For an extensive discussion, see the article by Ellis in this volume.

McGaugh (1994b) has shown that LSB disks with μ_0 ~ 23.5 mag arcsec^{-2} and s ~ 3 kpc can be readily detected by ultra-deep surveys out to z ~ 0.8, because the high sensitivity of CCD surveys more than compensates for cosmological dimming and k-corrections. However, a disk galaxy with the properties just described will only be detectable in the wide area survey of Loveday et al (1992) out to z = 0.02, with only one third of the flux is detected above the limiting isophote. Both the numbers and fluxes of LSB galaxies are underestimated by large area photographic surveys. To summarize, the optimum surface brightness for galaxy detection moves to higher *intrinsic* surface brightness with redshift, to counteract the effects of k-corrections and cosmological dimming. These distance-dependent selections effects can mimic evolutionary changes in the galaxy population and distort the observed luminosity function at high redshift.

Sprayberry et al (1997) carried out a morphological separation of the LSB galaxies with redshifts from the APM survey, of which ~ 50% are spirals and ~ 40% of which are irregulars (the remainder have peculiar morphologies). Most of the rise in the numbers fainter than M_B = - 16 is accounted for by irregulars. This joins a growing list of studies that find gas-rich irregulars to be a steeply rising component of the field galaxy luminosity function. Although the statistics are poor, Marzke et al (1994b) found a faint end slope of α = - 1.87 for the irregular Sm-Im types. Schade & Ferguson (1994) deduced α = - 1.63 for low luminosity star-forming galaxies, based on a reinterpretation of the survey of Salzer (1989, see also Boroson, Salzer & Trotter 1993). Driver et al (1994b) have suggested a dwarf-rich model to explain deep *BVRI* galaxy counts. The model with α = - 1.8 for the dwarfs can be used to fit the *B* band counts down to *B* = 27.5, but such a model predicts lower redshifts than are observed by spectroscopy down to *B* = 24 (Cowie, Songaila, & Hu 1991). More recently, Driver et al (1995a) have measured the morphologies of galaxies from a single ultradeep WFPC2 image. At a depth corresponding to $B \simeq 26$, half the galaxies are late-type spirals or irregulars, and find that some combination of rapid evolution and a steep faint end slope for the local dwarf luminosity function is required to account for the data.

The local low luminosity LSB population can be compared with the faint blue galaxies in the Medium Deep Survey (MDS) of Driver, Windhorst & Griffiths (1995b), which are taken to be at a typical redshift of $z \sim 0.3$. LSB field galaxies with $M_B > -16$, are at typical distances of $10 < d < 40 h_{100}^{-1}$ Mpc. They have central surface brightnesses in the range $22 < \mu < 25$ *B* mag arcsec^{-2} , and effective angular radii of $6 < r_{eff} < 20$ arcseconds (Impey et al 1996). If they are related to the LSB dwarfs in clusters, they will have $B - V \sim 0.5$ (Impey, Bothun & Malin 1988). The late-type and irregular (Sdm/Irr) MDS galaxies have median effective radii of 0.4 arcseconds (Im et al 1995a), which would scale to 20 arcseconds for a local population. The central surface brightnesses of the MDS sample convert into a range $23 < \mu < 24$ *B* mag arcsec^{-2} locally, assuming no evolution. The Sdm/Irr MDS galaxies have colors $V - I \sim 1$, also consistent with a local color of $B - V \sim 0.5$, again assuming no evolution. In addition, Dalcanton & Schectman (1996) showed that the faint blue "chain" galaxies found by Cowie, Hu & Songaila (1995b) can be plausibly related to edge-on LSB disk galaxies. Both the faint blue galaxies (Efstathiou et al 1991) and the local LSB galaxies (Mo et al 1994) are weakly clustered.

While it can be shown that local LSB galaxies have similar properties to many of the faint blue galaxies, it is not clear that the high and low redshift populations can be related with a consistent evolutionary scheme. All such comparisons must take account of the change in morphology with luminosity at any redshift, from luminous E/S0/Sp types down to dwarf E/S0/Im types. Detailed modelling is hampered by the factor of two disagreement between the normalizations of the deep survey luminosity functions (Ellis et al 1996, Cowie et al 1996), probably caused by large scale structure along the pencil-beam surveys. Generally speaking, deep redshift surveys point to two populations at $z \sim 0.5$: red galaxies that evolve very little, and a rapidly evolving (and presumably fading) blue population (Lilly et al 1996, Ellis et al 1996).

Ferguson & McGaugh (1995) have demonstrated that LSB galaxies could be a substantial contributor to the faint galaxy counts. They considered two rather extreme populations in the (μ, *L*) plane: galaxies with *L* and μ uncorrelated, and galaxies with a tight correlation between *L* and μ. Redshifts for the APM sample (Impey et al 1996) indicate that the truth lies between these two situations (see Figure 2). Babul & Ferguson (1996) have used plausible evolutionary models to make detailed predictions of faint blue galaxies that fade and redden, based on the earlier model of Babul & Rees (1992). There are a number of difficulties in identifying local LSB galaxies as the faded remnants of the faint blue galaxy population. If faded red galaxies are present in sufficient profusion, they should appear in the low redshift bins of the deep redshift surveys (Lilly et al 1995, Bouwens & Silk 1996), and they should contribute to the deep counts around *B* = 26 (Driver & Phillipps 1996). In addition, the nearby LSB population is too blue to fit a fading scenario, and the disks appear to be evolving slowly not rapidly (McGaugh 1994a, Ferguson & McGaugh 1995). Fading scenarios usually invoke supernova-driven gas ejection during a burst of star formation, in conflict with the large gas content of the local sample. The existing uncertainty strongly motivates new searches for dim and diffuse galaxies.

FORMATION OF LSB GALAXIES Finally, LSB galaxies can be placed in the context of galaxy formation and evolution in the broadest sense. Figure 7a shows a schematic version of the bivariate luminosity function of galaxies in stars (measured by luminosity and surface brightness for E galaxies) and gas (measured by the 21-cm line for Sp galaxies). The selection effects against finding extreme LSB galaxies like Malin 1 and the Virgo cloud (Giovanelli & Haynes 1989) are formidable. Since starbursting dwarfs do not have the gas supply to sustain their star formation for long, we might wonder how to detect the larger number of quiescent dwarfs. Our understanding of what drives the star formation history and visibility of galaxies, through the conversion of M_{HI} into M_B, is still very incomplete.

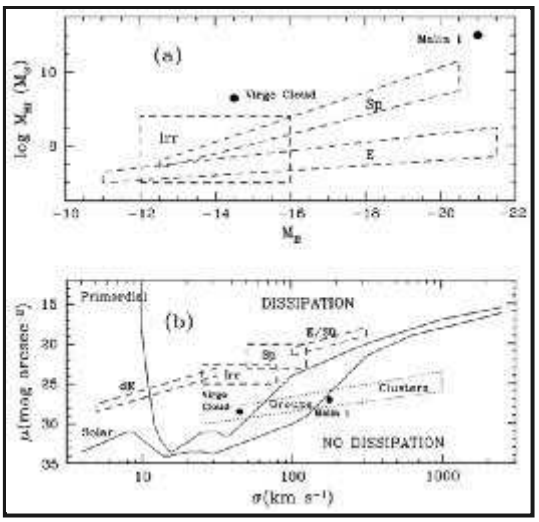

Figure 7. (a) Schematic plot of stellar luminosity against gas mass for different galaxy types. LSB galaxies of various types lie not far off the relationship defined by most galaxies. (From Giovanelli & Haynes 1989, Bothun et al 1987.) (b) Plot of surface brightness in the *B* band or surface mass density against velocity dispersion for various cosmic structures, assuming dissipation from intercloud collisions. The giant LSB disk galaxies have the dynamical properties of groups of galaxies. (From Efstathiou & Silk 1983, see also Burstein et al 1995.)

It appears that the formation of large numbers of LSB galaxies is an unavoidable consequence of heirarchical schemes for the formation of large scale structure. In the standard picture of the spherical collapse of a top-hat density perturbation (Gunn & Gott 1972), smaller perturbations reach their maximum extents more slowly, and collapse at later times. Assuming Gaussian fluctuations, small amplitude peaks will be found preferentially in under-dense regions, such that galaxies that result from small amplitude peaks are less correlated than galaxies that collapse earlier from large amplitude peaks (Kaiser 1984). It is natural to associate dwarf galaxies with the 1-2σ peaks (Dekel & Silk 1986). Mo, McGaugh & Bothun (1994) showed that the clustering properties of LSB galaxies were consistent with late formation. The giant, gas-rich galaxies like Malin 1 are more likely to originate from rare, 3σ peaks in under-dense regions, since the gas disks are vulnerable to interactions in over-dense regions (Hoffman, Silk & Wyse 1992).

In their application of the formalism of Press & Schechter (1974), Dalcanton, Spergel & Summers (1997a) find that the mean baryonic surface mass density $\bar{\Sigma} \propto Fr_\star \Lambda^3(\lambda)(\delta\rho/\rho)^3$ in the case $\Omega = 1$. The mean surface density is defined with a region of size $r_\star$, which has a collpase factor $\Lambda(\lambda)$, where λ is the dimensionless spin parameter. The timescale of violent relaxation and virialization is $\tau_{vir} \propto [(\delta\rho/\rho) + 1]$, and the virialized radius is $R_{vir} = R_{init}(1 + z)^{-1}(1 + 178\,\Omega^{-0.6})^{-1/3}$. Furthermore, the amplitude of the correlation function traced by galaxies is $\bar{\Sigma} \propto \Lambda^3(\lambda)\,\xi(r)^{3/2}$, so that the correlation amplitude of galaxies only falls as a weak function of surface mass density. This is consistent with the clustering amplitude of LSB galaxies measured by Mo, McGaugh & Bothun (1994). The total mass density of LSB galaxies in heirarchical clustering schemes can exceed the mass density of normal, high surface brightness galaxies.

Figure 7b shows the role that dissipation plays in structure formation in the universe (e.g. Efstathiou & Silk 1983). In this plot of surface brightness (or equivalently, surface mass density) versus velocity dispersion, the solid lines show the demarcation between structures that have undergone dissipation and those that have not. This simple model assumes that star formation occurs by radiative shocks in intercloud collisions. If either the surface mass density is too low or the velocity dispersion is too high, the cooling is inefficient and so there is no compression and no subsequent star formation. The stellar velocity dispersion is therefore a fossilized measure of the cloud velocity dispersion at the epoch when most of the dissipation (and star formation) occurred.

In heirarchical clustering, the relationship between surface mass density and velocity dispersion for non-dissipative structures is

$\bar{\Sigma} \propto \sigma^{-4(n+2)/(1-n)}$, where n is the spectral index of the initial fluctuations (Efstathiou & Silk 1983). Clustering goes towards increasing σ if $n < 1$, and towards increasing $\bar{\Sigma}$ if $n > -2$. The eventual goal is to understand LSB systems well enough to interpret them in terms of an "HR" diagram for galaxies, a goal that is being approached for dynamically hot systems (Bender, Burstein, & Faber 1993). This goal is plausible as long as the structure of the dissipative baryonic matter is directly related to the structure of the dark halo (Faber 1982). Figure 7a illustrates that extreme LSB galaxies like Malin 1 and the Virgo cloud have similar properties to small groups or clusters of galaxies (Burstein et al 1995). They are displaced by a factor of 100 in surface mass density from the conventional galaxies of the Hubble sequence. This suggests an alternate evolutionary history that involves late collapse and dissipation, slow evolution, and a low density cosmic environment.

LSB galaxies play a key role in this cosmogony. Navarro, Frenk & White (1996) argue that dark matter halos which formed through dissipationless heirarchical clustering have a universal mass profile. Each halo mass is specified solely by its characteristic overdensity, which depends on the mean density at the epoch of collapse. HSB galaxies have fast-rising rotation curves which flatten off to outer regions of dark matter domination. LSB disks have slowly rising rotation curves that are dark matter dominated at almost all radii. Pickering et al (1997) show examples that can be traced out to ~ 100 h_{100}^{-1} kpc. In general, LSB galaxies have high angular momentum disks, with larger scale lengths at the same circular velocity (Zwaan et al 1995). Dalcanton, Spergel & Summers (1997a) describe the evolution of high angular momentum, low surface mass density disks, and provide a context for understanding the broad relationship between luminosity and surface brightness, and for understanding the properties of the local luminosity function. Moreover, the Cold Dark Matter model predicts far too many dark halos to match the cataloged galaxy population (White & Frenk 1991). Many dark halos may have failed to form galaxies, or may have formed galaxies that have so far escaped detection. Observational limitations and theoretical expectations align to point to the importance of LSB galaxies.

ACKNOWLEDGMENTS

We acknowledge inspiration and provocation from our former students, Stacy McGaugh and David Sprayberry, our current students, Tim Pickering and Karen O'Neil, and our longtime collaborators, Jim Schombert and David Malin. A number of colleagues contributed greatly to the results and ideas described in this review - Bruno Binggeli, Frank Briggs, Julianne Dalcanton, Simon Driver, Harry Ferguson, Mike Irwin, Pat Knezek, Ron Marzke, Allan Sandage, and Steve Schneider. We are grateful to the Welsh "dragons," Mike Disney, Steve Phillipps, and Jon Davies, for breathing life and fire into this subject over a number of years. Allan Sandage is thanked for his many detailed and thoughtful comments on the manuscript. We acknowledge support from the NSF under grant AST-9003158.

REFERENCES

1. Allen R, Shu F. 1979. *Ap. J.* 227:67
2. Arp HC. 1965. *Ap. J.* 142:402
3. Babul A, Rees MJ. 1989. *MNRAS* 255:346
4. Babul A, Ferguson HC. 1996. *Ap. J.* 458:100
5. Bahcall JN, Bergeron J, Boksenberg A, Hartig GF, Jannuzi BT, et al. 1993. *Ap. J. Suppl.* 87:1
6. Bender R, Burstein D, Faber SM. 1993. *Ap. J.* 411:153
7. Bergeron J. 1995. In *ESO Workshop on Quasar Absorption Lines.*, ed. G Meylan, in press, p. 127-136. Dordrecht: Springer-Verlag
8. Bergeron J, Boisse P. 1991. *Astron. Astrophys.* 243:344
9. Bernstein GM, Nichol RG, Tyson AJ, Ulmer MP, Wittman D. 1995. *Astron. J.* 110:1507
10. Bershady MA, SubbaRao MU, Szalay A, Koo DC, Kron RG, Hereld M. 1997. Submitted to *Ap. J.*
11. Binggeli B, Sandage A, Tarenghi M. 1984. *Astron. J.* 89:64
12. Binggeli B, Sandage A, Tammann GA. 1985. *Astron. J.* 90:1681
13. Binggeli B, Sandage A, Tammann GA. 1988. *Annu. Rev. Astron. Astrophys.* 26:509
14. Binggeli B, Tarenghi M, Sandage A. 1990. *Astron. Astrophys.* 228:42
15. Boroson TA. 1981. *Ap. J. Suppl.* 46:177
16. Boroson TA, Salzer JJ, Trotter A. 1993. *Ap. J.* 412:524
17. Bothun GD, 1985. *Astron. J.* 90:1982
18. Bothun GD, Impey CD, Malin DF, Mould JR. 1987. *Astron. J.* 94:23
19. Bothun GD, Schombert JM., Impey CD, Schneider SE. 1990. *Ap.J.* 360:427
20. Bothun GD, Impey CD, Malin DF. 1991. *Ap. J.* 376:404
21. Bosma A, Freeman KC. 1993. *Astron. J.* 106:1394
22. Bouwens RJ, Silk J. 1996. *Ap. J. Lett.* 471:L19
23. Briggs FH. 1990. *Astron. J.* 100:999
24. Bristow PD, Phillipps S. 1994. *MNRAS* 267:13

25. Broadhurst TJ, Ellis RS, Shanks TS. 1988. *MNRAS* 235:827
26. Broeils AH. 1992. *Dark and Visible Mass in Spiral Galaxies.* Ph.D. Thesis. University of Groningen
27. Bruzual GA, Charlot S. 1993. *Ap. J.* 405:538
28. Burstein D, Bender R, Faber SM, Nolthenius R. 1995. *Astron. Lett. Comm.* 31:95
29. Caldwell N, Bothun GD. 1987. *Astron. J.* 94:1126
30. Capaccioli A, de Vaucouleurs G. 1983. *Ap. J. Suppl.* 52:465
31. Carr BJ. 1994. *Annu. Rev. Astron. Astrophys.* 32:531
32. Cayette V, Kotanyi C, Balkowski C. 1993. *Astron. J.* 107:1003
33. Cen R, Miralda-Escude J, Ostriker JP, Rauch M. 1994. *Ap. J. Lett.* 437:L9
34. Cole S, Treyer M, Silk J. 1992. *Ap. J.* 385:9
35. Copi CJ, Schramm DN, Turner MS. 1995. *Sci* 267:192
36. Corbelli E, Salpeter, EE. 1993. *Ap. J.* 419:104
37. Courteau S. 1996. *Ap. J. Suppl.* 103:363
38. Cowie LL. 1988. In *The Post-Recombination Universe*, eds. N Kaiser, A Lazenby, p. 1-18. Dordtrect: Kluwer
39. Cowie LL, Songaila A, Hu EM. 1991. *Nature* 354:460
40. Cowie LL, Hu EM, Songaila A. 1995a. *Nature* 377:603
41. Cowie LL, Hu EM, Songaila A. 1995b. *Astron. J.* 109:1522
42. Cowie LL, Songaila A, Hu EM, Cohen JG. 1996. *Astron. J.* 112:839
43. da Costa G, Nicolaci L, Geller MJ, Pellegrini PS, Latham DW, et al. 1994. *Ap. J. Lett.* 424:1
44. Dalcanton JJ. 1993. *Ap. J. Lett.* 415:L87
45. Dalcanton JJ. 1995. *The Nature of Ultra-Low Surface Brightness Objects.* Ph.D. Thesis. University of Princeton
46. Dalcanton JJ, Schectman SA. 1996. *Ap. J. Lett.* 465:L9
47. Dalcanton JJ, Spergel DN, Summers FJ. 1997a. *Ap. J.* 482: 659
48. Dalcanton JJ, Spergel DN, Gunn JE, Schmidt M, Schneider DP. 1997b. *Astron. J.* 114: 635
49. Davies JI. 1990. *MNRAS* 244:8
50. Davies JI, Phillipps S, Cawson MGM, Disney MJ, Kibblewhite EJ. 1988. *MNRAS* 232:239
51. Davies JI, Phillipps S, Disney MJ. 1990. *MNRAS* 244:385
52. Dekel A, Silk J. 1986. *Ap. J.* 303:39
53. de Blok WJG, van der Hulst JM, Bothun GD. 1995. *MNRAS* 274:235
54. de Blok WJG, McGaugh, SS, van der Hulst JM. 1996. *MNRAS* 283:18
55. de Jong RS. 1995. *Spiral Galaxies: the light and color distributions in the optical and near-infrared.* Ph.D. Thesis. University of Groningen
56. de Jong RS, van der Kruit PC. 1994. *Astro. Astrophys. Suppl.* 106:451
57. de Propris R, Pritchet CJ, Harris WE, McClure RD. 1995. *Ap. J.* 450:534
58. de Vaucouleurs G, de Vaucouleurs A, Corwin HG, Buta R, Paturel G, Fouque P. 1991. *Third Reference Catalog of Bright Galaxies.* New York: Springer-Verlag
59. Dinshaw N, Foltz CB, Impey CD, Weymann RJ, Morris SL. 1995. *Nature* 373:223
60. Disney MJ. 1976. *Nature* 263:573
61. Disney MJ, Phillipps S. 1983. *MNRAS* 205:1253
62. Disney MJ, Banks G. 1997. Submitted to *MNRAS*
63. Dove JB, Shull JM. 1994. *Ap. J.* 423:196
64. Driver SP, Phillipps S, Davies JI, Morgan I, Disney MJ. 1994a. *MNRAS* 268:393
65. Driver SP, Phillipps S, Davies JI, Morgan I, Disney MJ. 1994b. *MNRAS* 266:155
66. Driver SP, Windhorst RA, Ostrander EJ, Keel WC, Griffiths RE, Ratnatunga KU. 1995a. *Ap. J. Lett.* 449:L23
67. Driver SP, Windhorst RAW, Griffiths RE. 1995b. *Ap. J.* 453:48
68. Driver SP, Phillipps S. 1996. *Ap. J.* 469:529
69. Ellis RS, Colless M, Broadhurst T, Heyl J, Glazebrook K. 1996. *MNRAS* 280:235
70. Efstathiou G, Silk J. 1983. *Fundamentals of Cosmic Physics* 9:1
71. Efstathiou G, Ellis RS, Peterson BA. 1988. *MNRAS* 232:431
72. Efstathiou G, Bernstein G, Tyson JA, Katz N, Guhathakurta P. 1991. *Ap. J. Lett.* 380:L47
73. Faber SM. 1982. In *Astrophysical Cosmology* ed. HA Bruck, GV Coyne, MS Longair, p. 191-215, Vatican: Pontifica Academia Scientarium
74. Felten JE. 1977. *Astron. J.* 82:861
75. Ferguson HC. 1989. *Astron. J.* 98:367
76. Ferguson HC, Sandage A. 1988. *Astron. J.* 96:1520
77. Ferguson HC, Binggeli B. 1994. *Astron. Astrophys. Rev.* 6:67
78. Ferguson HC, McGaugh SS. 1995. *Ap.J.* 440:470
79. Fish RA. 1964. *Ap. J.* 139:284
80. Fisher JR, Tully RB. 1975. *Astron. Astrophys.* 44:151
81. Fisher JR, Tully RB. 1977. *Ap. J. Lett.* 243:23
82. Fisher JR, Tully RB. 1981. *Ap. J. Suppl.* 47:139

83. Freedman WL, Madore BF, Kennicutt RC. 1997. In *The Extragalactic Distance Scale.* ed. M Livio, M Donohue, N Panagia, Cambridge: Cambridge University Press, in press
84. Freeman KC. 1970. *Ap. J.* 160:811
85. Fukagita M, Turner EL. 1991. *MNRAS* 253:99
86. Gallagher JS, Hunter DA. 1984. *Annu. Rev. Astron. Astrophys.* 22:37
87. Giovanelli R, Haynes MP. 1989. *Astron. J.* 97:633
88. Giovanelli R, Haynes MP. 1989. *Ap. J. Lett.* 346:L5
89. Grogin NA, Narayan R. 1996. *Ap. J.* 464:92
90. Gunn JE, Knapp GR. 1993. In *Sky Surveys: Protostars to Protogalaxies.* ed. BT Soifer, p. 267-280, San Francisco: Astronomical Society of the Pacific
91. Gunn JE, Gott JR. 1972. *Ap. J.* 176:1
92. Harrison ER. 1964. *Nature* 204:271
93. Hawarden TG, Longmore AJ, Goss WM, Mebold U, Tritton SB. 1981. *MNRAS* 196:175
94. Hernquist L, Katz N, Weinberg DH, Miralda-Escude J. 1996. *Ap. J. Lett.* 457:L51
95. Hoffman GL, Lewis BM. Helou G, Salpeter EE, Williams HL. 1989. *Ap. J. Suppl.* 69:65
96. Hoffman Y, Silk J, Wyse RFG. 1992. *Ap. J. Lett.* 388:13
97. Holmberg E. 1975. In *Stars and Stellar Systems, Vol. 9.* ed. A Sandage, M Sandage, J Kristian, p. 123, Chicago: University of Chicago Press
98. Hubble E. 1936. In *The Realm of the Nebulae.* New Haven, Conn: Yale University Press
99. Im M, Casretano S, Griffiths RE, Ratnatunga JU, Tyson JA. 1995a. *Ap. J.* 441:494
100. Im M, Ratnatunga KU, Griffiths RE, Casertano S. 1995b. *Ap. J. Lett.* 445:15
101. Impey CD, Bothun GD, Malin DF. 1988. *Ap. J.* 330:634
102. Impey CD, Bothun GD. 1989. *Ap.J* 341:89
103. Impey CD, Sprayberry D, Irwin MJ, Bothun GD. 1996. *Ap. J. Suppl.* 105:209
104. Irwin MJ, Davies JI, Disney MJ, Phillipps S. 1990a. *MNRAS* 245:289
105. Irwin MJ, Bunclark PS, Bridgeland MT, McMahon RG. 1990b. *MNRAS* 244:16P
106. Irwin MJ, Hatzidimitriou D. 1995. *MNRAS* 277:1354
107. Kaiser N. 1984. *Ap. J. Lett.* 284:L9
108. Kennicutt RC. 1983. *Ap. J.* 272:54
109. Kennicutt RC. 1989. *Ap. J.* 344:685
110. Knezek PM. 1993. *The Stellar and Gaseous Content of Massive Low Surface Brightness Galaxies.* Ph.D. Thesis. University of Massachusetts
111. Koo DC, Gronwall C, Bruzual G. 1993. *Ap. J. Lett.* 415:L21
112. Kormendy J. 1977. *Ap. J.* 217:406
113. Kormendy J. 1985. *Ap. J.* 295:73
114. Kron RG. 1982. *Vistas in Astronomy* 26:37
115. Lanzetta KM. Wolfe AM, Turnshek DA, Lu L, McMahon RG, Hazard C. 1991. *Ap. J. Suppl.* 77:1
116. Lanzetta KM, Wolfe AM, Turnshek DA. 1995. *Ap. J.* 440:435
117. Lilly SJ, Cowie LL, Gardner JP. 1991. *Ap. J.* 369:79
118. Lilly SJ. 1993. *Ap. J.* 411:501
119. Lilly SJ, LeFevre O, Hammer F, Crampton D. 1996. *Ap. J. Lett.* 460:1
120. Lin H, Kirshner RP, Schectman SA, Landy SD, Oemler A. 1996. *Ap. J.* 464:60
121. Longmore AJ, Hawarden TG, Goss WM, Mebold U, Webster BL. 1982. *MNRAS* 200:325
122. Loveday J, Peterson BA, Efstathiou G. Maddox SJ. 1992. *Ap. J.* 390:338
123. Malaney P, Mathews G. 1993. *Phys. Rep.* 229:147
124. Malin DF. 1978. *Nature* 276:591
125. Maloney P. 1993. *Ap.J.* 414:41
126. Marzke RO, Huchra JP, Geller MJ. 1994a. *Ap. J.* 428:43
127. Marzke RO, Geller MJ, Huchra JP, Corwin Jr HG. 1994b. *Astron. J.* 108:437
128. Marzke RO, da Costa LN. 1997. *Astron. J.* 113:185
129. Mateo M. 1996. In *Formation of the Galactic Halo, Inside and Out.* ed. H Morrison, A Sarajedini, p. 434. San Francisco: Astron. Soc. Pac.
130. Mattila K. 1990. In *The Galactic and Extragalactic Background Radiation.* ed. S Bowyer, C Leinert, p. 257, Dordrecht: Kluwer
131. Mattila K, Leinart Ch, Schnur G. 1991. In *The Early Observable Universe from Diffuse Backgrounds.* ed. B Rocca-Volmerange, JM Deharvang, J Tran Thanh Van, p. 133. Editions Frontieres
132. McGaugh SS. 1992. *The Physical Properties of Low Surface Brightness Galaxies.* Ph.D. Thesis. University of Michigan, Ann Arbor
133. McGaugh SS. 1994a. *Ap. J.* 426:135
134. McGaugh SS. 1994b. *Nature* 367:538
135. McGaugh SS, Bothun GD. 1994. *Astron. J.* 107:530

136. McGaugh SS, Bothun GD, Schombert JM. 1995. *Astron. J.* 110:573
137. McGaugh SS. 1996. *MNRAS* 280:337
138. Meurs EJA, Wilson AS. 1984. *Astron. Astrophys.* 136:206
139. Meylan G. 1995. Editor, *ESO Workshop on Quasar Absorption Lines.* Dordrecht: Springer-Verlag, in press
140. Mo HJ, McGaugh SS, Bothun GD. 1994. *MNRAS* 267:129
141. Morgan I, Driver SP. 1995. In *Extragalactic Background Radiation.* ed. D Calzetti, M Livio, P Madau, p. 285-288. Cambridge: Cambridge University Press
142. Morris SL, Weymann RJ, Savage BD, Gilliland RL. 1991. *Ap. J. Lett.* 377:L21
143. Nilson PN. 1973. *Uppsala General Catalog of Galaxies.* Uppsala, Finland: Uppsala Astronomical Observatory
144. O'Connell RW. 1987. *Astron. J.* 94:876
145. O'Neil K, Bothun GD, Smith EP, Stecher TP. 1996. *Astron. J.* 112:431
146. O'Neil K, Bothun GD, Cornell M, Impey CD. 1997. Submitted to *Astron. J.*
147. Peebles PJE, Schramm D, Turner E, Kron R. 1991. *Nature* 352:769
148. Peebles PJE. 1993. In *Principles of Physical Cosmology.* p. 391. Princeton:Princeton University Press
149. Persic M, Salucci P. 1990. *MNRAS* 245:577
150. Persic M, Salucci P. 1992. *MNRAS* 258:14P
151. Petitjean P, Mucket JP, Kates RE. 1995. *Astron. Astrophys.* 295:L9
152. Phillipps S, Fong R, Shanks T. 1981. *MNRAS* 194:49
153. Phillipps S, Disney MJ. 1985. *Astron. Astrophys.* 148:234
154. Phillipps S, Disney MJ, Kibblewhite EJ, Cawson MG. 1987. *MNRAS* 229:505
155. Phillipps S, Driver SP. 1995. *MNRAS* 274:832
156. Phillipps S, Davies JI, Disney MJ. 1990. *MNRAS* 242:235
157. Phillipps S, Disney MJ, Davies JI. 1993. *MNRAS* 260:453
158. Pickering TE, Impey CD, van Gorkom J, Bothun GD. 1997. *Ap. J.* 114: 1858
159. Press WH, Schechter PL. 1974. *Ap. J.* 330:579
160. Quirk WJ. 1972. *Ap. J. Lett.* 176:9
161. Rao SM, Briggs FH. 1993. *Ap.J.* 419:515
162. Rao SM, Turnshek DA, Briggs FH. 1995. *Ap. J.* 449:488
163. Rauch M, Haehnelt MG. 1995. *MNRAS* 275:L76
164. Rauch M, Weymann RJ, Morris SL. 1996. *Ap. J.* 458:518
165. Reaves G. 1956. *Astron. J.* 61:69
166. Romanishin W, Krumm N, Salpeter E, Knapp G, Strom KM, Strom SE. 1982. *Ap. J.* 263:94
167. Romanishin W, Strom KM, Strom SE. 1983. *Ap. J. Suppl.* 53: 105
168. Saha A, Sandage A, Labhardt L, Tammann GA, Macchetto FD, Panagia N. 1996. *Ap. J. Suppl.* 107:693
169. Salzer JJ. 1989. *Ap. J.* 347:152
170. Sandage A, Tammann G, Yahil A. 1979. *Ap. J.* 232:352
171. Sandage A, Binggeli B, Tammann GA. 1985. *Astron. J.* 90:1759
172. Sandage A. 1988. *Annu. Rev. Astron. Astrophys.* 26:561
173. Sargent WLW, Steidel CC, Boksenberg A. 1988. *Ap. J.* 334:22
174. Schade DJ, Ferguson HC. 1994. *MNRAS* 267:889
175. Schechter P. 1976. *Ap. J.* 203:297
176. Schectman SA. 1973. *Ap .J.* 188:233
177. Schectman SA. 1974. *Ap. J.* 179:681
178. Schombert JM, Bothun GD. 1988. *Astron. J.* 95:1389
179. Schombert JM. Bothun GD, Schneider SE, McGaugh SS. 1992. *Astron. J.* 103:1107
180. Schombert JM, Pildis RA, Eder JA, Oemler A. 1995. *Astron. J.* 110:2067
181. Schneider SE, Thuan TX, Magri C, Wadiak JE. 1990. *Ap. J. Suppl.* 72:245
182. Schneider SE, Thuan TX, Magnum JG, Miller J. 1992. *Ap. J. Suppl.* 81:5
183. Schneider SE. 1996. In *Minnesota Lectures on Extragalactic HI.* ed. E Skillman, p. 323-348. San Francisco: Astron. Soc. Pac.
184. Schwartzenberg JM, Phillipps S, Smith RM, Couch WJ, Boyle BJ. 1995a. *MNRAS* 275:121
185. Schwartzenberg JM, Phillipps S, Parker QA. 1995b. *Astron. Astrophys.* 293:332
186. Sprayberry D, Impey CD, Irwin MJ, McMahon RG, Bothun GD. 1993. *Ap. J.* 417:114
187. Sprayberry D, Impey CD, Bothun GD, Irwin MJ. 1995a. *Astron. J.* 109:558
188. Sprayberry D, Bernstein GM, Impey CD, Bothun GD. 1995b. *Ap. J.* 438:72
189. Sprayberry D, Impey CD, Irwin MJ. 1996. *Ap. J.* 463:535
190. Sprayberry D, Impey CD, Irwin MJ, Bothun GD. 1997. *Ap. J.*, 482: 104
191. Steidel CC, Sargent WLW. 1992. *Ap. J. Suppl.* 80:1
192. Steidel CC, Dickinson M. 1992. *Ap. J* 394:81
193. Steidel CC. 1993. In *The Evolution of Galaxies and Their Environment, 3rd Teton Summer School*, ed. JM Shull, H Thronson, p. 263-294. Dordtrecht: Kluwer

194. Storrie-Lombardi LJ, McMahon RG, Irwin MJ, Hazard C. 1994. *Ap. J. Lett.* 427:L13
195. Szomoru A, Guhathakurta P, van Gorkom JH, Knapen JH, Weinberg DH, Fruchter AS. 1994. *Astron. J.* 108:491
196. Toomre A. 1964. *Ap. J* 139:1217
197. Trentham N. 1997. *MNRAS* in press
198. Turner JA, Phillipps S, Davies JI, Disney MJ. 1993. *MNRAS* 261:39
199. Tyson AJ. 1988a. *Astron. J.* 96:1
200. Tyson AJ. 1995. In *Extragalactic Background Radiation.* ed. D Calzetti, M Livio, P Madau, p. 103-128. Cambridge: Cambridge University Press
201. Tyson AJ, Jarvis JF. 1979. *Ap. J. Lett.* 230:L153
202. Tyson ND. 1988b. *Ap. J. Lett.* 329:L57
203. Tyson ND, Scalo JM. 1988. *Ap. J.* 329:618
204. Väisänen P. 1996. *Astron. Astrophys.* 315:21
205. van den Bergh S. 1959. *Publ. David Dunlap Obs.* 2:147
206. van der Hulst JM, Skillman, ED, Smith TR, Bothun GD, McGaugh SS, de Blok, WJG. 1993. *Astron. J.* 106:548
207. van der Kruit PC. 1987. *Astron. Astrophys.* 173:59
208. van Gorkom J, Cornwell T, van Albada TS, Sancisi R. 1997. ApJ, in press
209. Walker TP, Steigman G, Schramm DN, Olive KA, Kang H-S. 1991. *Ap. J.* 376:51
210. Warmels RH. 1985. *HI Properties of Spiral Galaxies in the Virgo Cluster.* Ph.D. Thesis. Groningen University
211. Weinberg DH, Szomoru A, Guhathakurta P, van Gorkom JH. 1991. *Ap. J. Lett.* 372:L13
212. White SDM, Frenk CS. 1991. *Ap. J.* 379:52
213. White SDM, Navarro JF, Evrard AE, Frenk CS. 1993. *Nature* 366:429
214. Wright EL. 1985. *Publ. Astron. Soc. Pac.* 97:451
215. York DG, Dopita M, Green RF, Bechtold JB. 1986. *Ap. J.* 311:610
216. Zucca E. 1997. In *37th Herstmonceux Conference on HST and the High Redshift Universe*, ed. M Pettini. Cambridge: Cambridge University Press, in press
217. Zwaan MA, van der Hulst JM, de Blok WJG, McGaugh SS. 1995. *MNRAS* 273:L35
218. Zwicky F. 1957. In *Morphological Astronomy.* New York: Springer-Verlag